High-Definition Fiber Tractography of the Human Brain: Neuroanatomical Validation and Neurosurgical Applications

Juan C. Fernandez-Miranda, MD*
Sudhir Pathak, MS, MSc‡
Johnathan Engh, MD*
Kevin Jarbo, BS‡
Timothy Verstynen, PhD‡
Fang-Cheng Yeh, MD, PhD§
Yibao Wang, MD*
Arlan Mintz, MD*
Fernando Boada, MD, PhD‖
Walter Schneider, PhD*‡
Robert Friedlander, MD*

*Department of Neurological Surgery and ‖Magnetic Resonance Research Center, Department of Radiology, University of Pittsburgh School of Medicine, University of Pittsburgh Medical Center, Pittsburgh, Pennsylvania; ‡Learning and Research Development Center, Department of Psychology, University of Pittsburgh, Pittsburgh, Pennsylvania; §Carnegie Mellon University, Department of Biomedical Engineering, Pittsburgh, Pennsylvania

Correspondence:
Juan C. Fernandez-Miranda, MD,
Department of Neurological Surgery,
University of Pittsburgh School of Medicine, University of Pittsburgh Medical Center,
200 Lothrop St, PUH B-400,
Pittsburgh PA 15213.
E-mail: fernandezmirandajc@upmc.edu

Received, August 20, 2011.
Accepted, March 7, 2012.
Published Online, April 17, 2012.

BACKGROUND: High-definition fiber tracking (HDFT) is a novel combination of processing, reconstruction, and tractography methods that can track white matter fibers from cortex, through complex fiber crossings, to cortical and subcortical targets with subvoxel resolution.

OBJECTIVE: To perform neuroanatomical validation of HDFT and to investigate its neurosurgical applications.

METHODS: Six neurologically healthy adults and 36 patients with brain lesions were studied. Diffusion spectrum imaging data were reconstructed with a Generalized Q-Ball Imaging approach. Fiber dissection studies were performed in 20 human brains, and selected dissection results were compared with tractography.

RESULTS: HDFT provides accurate replication of known neuroanatomical features such as the gyral and sulcal folding patterns, the characteristic shape of the claustrum, the segmentation of the thalamic nuclei, the decussation of the superior cerebellar peduncle, the multiple fiber crossing at the centrum semiovale, the complex angulation of the optic radiations, the terminal arborization of the arcuate tract, and the cortical segmentation of the dorsal Broca area. From a clinical perspective, we show that HDFT provides accurate structural connectivity studies in patients with intracerebral lesions, allowing qualitative and quantitative white matter damage assessment, aiding in understanding lesional patterns of white matter structural injury, and facilitating innovative neurosurgical applications. High-grade gliomas produce significant disruption of fibers, and low-grade gliomas cause fiber displacement. Cavernomas cause both displacement and disruption of fibers.

CONCLUSION: Our HDFT approach provides an accurate reconstruction of white matter fiber tracts with unprecedented detail in both the normal and pathological human brain. Further studies to validate the clinical findings are needed.

KEY WORDS: Cavernoma, DTI, Fiber tracking, Glioma, Human connectome, White matter

Neurosurgery 71:430–453, 2012 DOI: 10.1227/NEU.0b013e3182592faa www.neurosurgery-online.com

Nearly 2 decades ago, Crick and Jones[1] wrote that "to interpret the activity of living human brains, their neuroanatomy must be known in detail. New techniques to do this are urgently needed, since most of the methods now used on monkeys cannot be used on humans." The introduction of diffusion tensor imaging (DTI) a decade ago represented a major step toward this goal.[2,3] The ability to noninvasively map fiber tracts in the living human brain facilitated numerous applications in the diagnosis and treatment of brain disorders. The National Institute of Health Blueprint for Neuroscience Research stated that the Human Connectome Project is one of the great scientific challenges for the upcoming decade and has made a major investment in brain connection mapping.[4]

Several authors have demonstrated that DTI tractography provides accurate reconstruction of the major stem of white matter tracts, in agreement with classic and contemporary neuroanatomical studies.[5,6] Consequently, DTI has

ABBREVIATIONS: DSI, diffusion spectrum imaging; **DTI,** diffusion tensor imaging; **HDFT,** high-definition fiber tractography

TABLE 1. List of Neurosurgical Cases Studied With High-Definition Fiber Tractography

Type of Cases	n (n = 36)
High-grade gliomas	16
Low-grade gliomas	7
Cavernomas	5
Miscellaneous	
Metastasis	2
Meningiomas	2
Dermoid cyst	2
Colloid cyst	2

been incorporated into the diagnostic neurosurgical armamentarium, allowing for the first time the study of the spatial relationship of intracerebral lesions within the white matter tracts. Several authors have reported the utility of this technique for preoperative and even intraoperative localization of the pyramidal tract,[7-11] primary motor area,[12] optic radiations,[13] and language pathways.[14,15] DTI may improve preservation of eloquent regions during surgery by providing access to direct connectivity information between functional regions of the brain, and it has progressively been incorporated into strategic planning for resection of complex brain lesions.[15]

DTI, however, is unable to solve the crossing of fibers (the crossing problem) and to determine with accuracy the origin and destination of fibers (the termination problem), producing multiple artifacts and false tracts.[16,17] Diffusion-based deterministic MRI methods cannot at present reliably replicate many basic neuroanatomical features described more than a century ago by means of fiber dissection and histological techniques.[6,18,19] The crossing and termination problems are accentuated in the analysis of fiber tracts in the periphery of a brain lesion with mass effect and surrounding edema, significantly decreasing the accuracy of the technique in the clinical setting.[6,20]

New fiber mapping techniques such as high-angular-resolution diffusion imaging and diffusion spectrum imaging (DSI) have been developed to solve the limitations of DTI. High-angular-resolution diffusion imaging has better angular resolution and smaller voxels.[21] DSI measures diffusion spectra, thus enabling resolution of intravoxel heterogeneity of diffusion and resolves not the average direction, such as in DTI, but a set of directions of multiple pathways within the voxel.[22] These are important improvements that partially solve previous limitations and show qualitative matches to a few expected neuroanatomy features in primates[23] and humans.[18] Schmahmann et al[23] compared DSI with radiographic techniques and stated that the techniques were in good agreement, specifically, "By replicating the major features of these tracts identified by histological techniques in monkey, we show that DSI has the potential to cast new light on the organization of the human brain in the normal state and in clinical disorders."

For the last 3 years, we have been applying high-angular-resolution diffusion imaging and DSI techniques to the study of structural brain connectivity in normal subjects and patients with brain lesions. The strengths and limitations of these techniques were identified.[24] In an attempt to more effectively solve the crossing and termination problems, we have focused on optimizing these methods to obtain what we refer to as high-definition fiber tracking (HDFT). HDFT is a novel combination of processing, reconstruction, and tractography methods that can track fibers from cortex, through complex fiber crossings, to cortical and subcortical targets with at least millimeter resolution. This is in contrast to low directional methods such as DTI in which such resolution is not accessible. HDFT relies on the unique combination of several factors: dense sampling of region of interest–based tractography data, generalized Q-ball imaging reconstruction algorithm, multiple intravoxel sampling, and a multidirectional

TABLE 2. High-Definition Fiber Tractography in the Normal Brain: Replication of Known Neuroanatomical Features

Neuroanatomical Feature	Neuroanatomical Region	Neuroanatomical Replication	Figure
Cortical termination	Hemispheric surface	Sulcal and gyral pattern	1 and 2
Subcortical termination	Claustrocortical projection system	Ovoid shape of claustrum	3
Subcortical termination and subcortical fiber-based segmentation	Thalamocortical projection system	Somatotopy of thalamic radiations	4
Double subcortical termination and decussation of fibers	Superior cerebellar peduncle	Characteristic shape of dentate and red nuclei; partial decussation of fibers	5
Triple crossing	Centrum semiovale	Multidirectional crossing of callosal, arcuate, and corona radiata fibers	6
Complex angulations	Meyers loop	Anterograde loop of optic radiations	7
Arborization of terminal fibers and multiple cortical terminations	Arcuate fascicle	Branching pattern of the arcuate tract at the frontal and temporal regions	8
Cortical connectivity and segmentation	Broca area	Segmentation of Broca area based on fiber connectivity	9

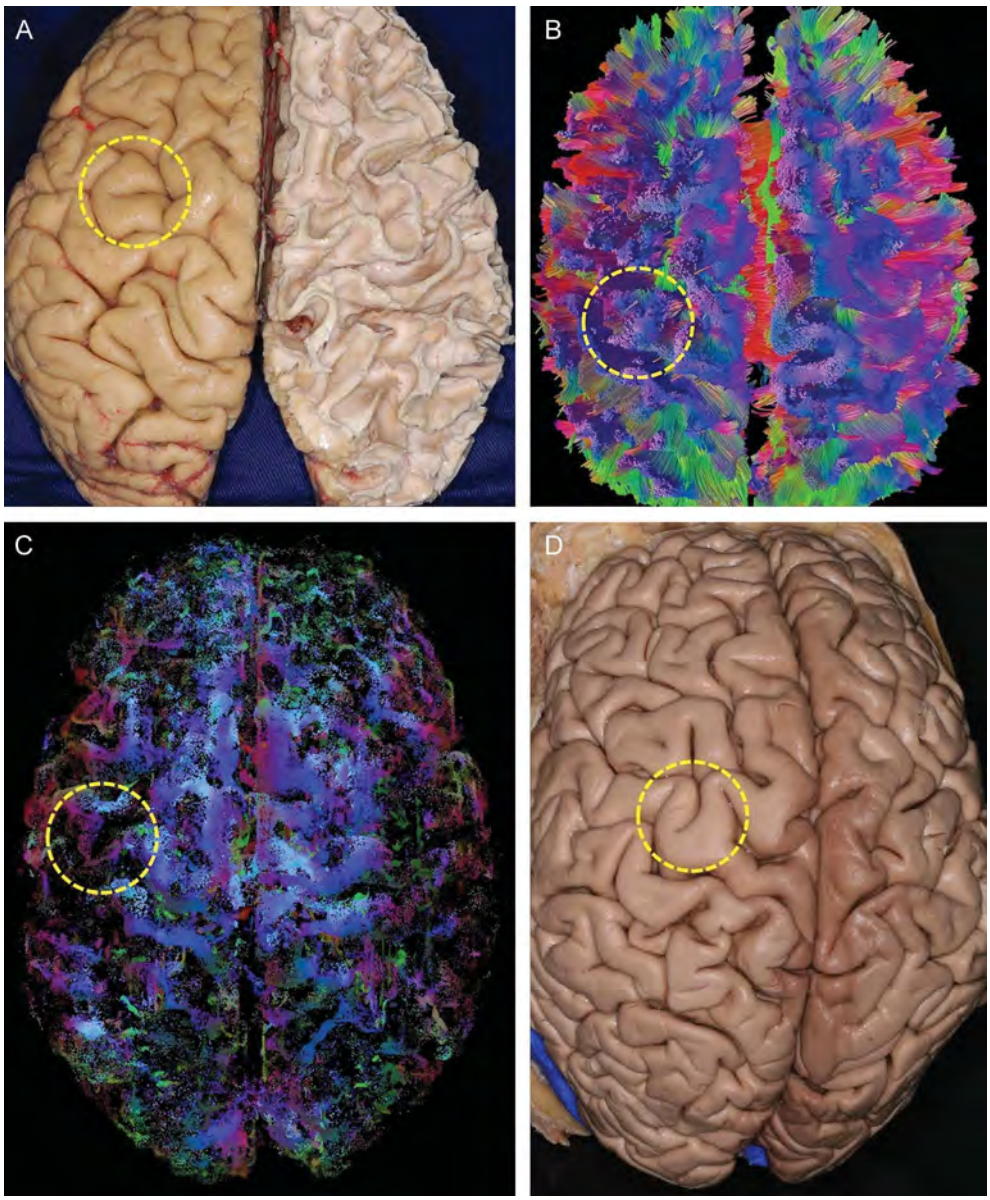

FIGURE 1. *Cortical termination of the fibers.* **A**, *anatomical specimen, superior view; the cortical surface of the right hemisphere has been dissected to show the underlying white matter structure.* **B**, *high-definition fiber tractography (HDFT) showing the white matter fibers of the whole brain.* **C**, *HDFT showing the end points of the whole brain fibers.* **D**, *anatomical specimen; superior view of the cortical surface to correlate with* **B** *and* **C**. *The yellow interrupted circle shows the location of the Ω-shaped motor hand area in* **A** *through* **D**. *Fibers and end points in* **B** *and* **C**, *respectively, are color coded by direction (eigenvector orientation): red, left to right; green, anterior to posterior; and blue, inferior to superior. Intermediate colors reflect intermediate ("oblique") directions.*

version of Fiber Assignment by Continuous Tracking deterministic tractography implemented in DSI-Studio.[25-31]

The first objective of this article is to present our results with the application of HDFT for the study of structural connectivity in normal subjects, aiming to demonstrate that HDFT is able to replicate known neuroanatomical features when current methods fail. For this purpose, we compare our HDFT reconstructions in normal subjects with precise white fiber anatomical microdissection in human brains. Second, we present our experience with the clinical application of HDFT for the presurgical analysis and

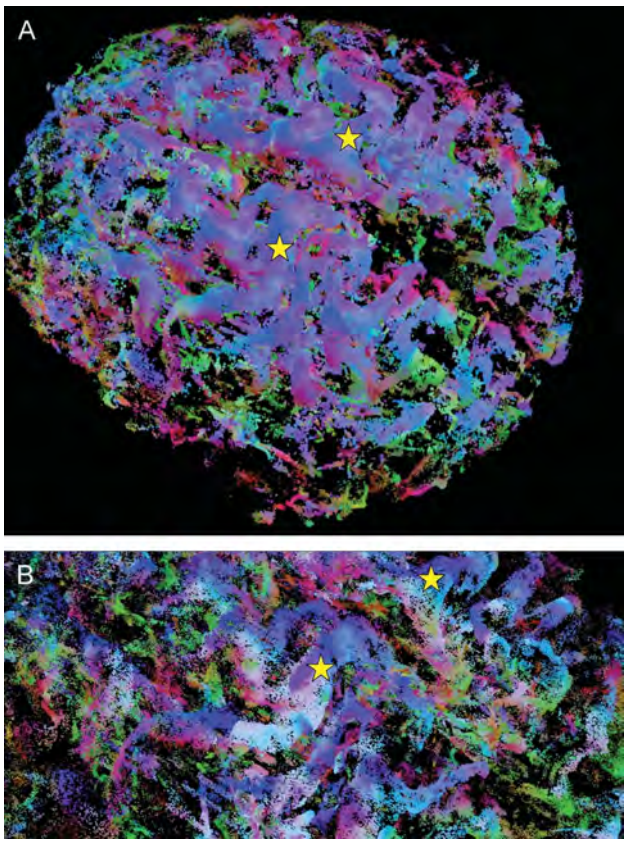

FIGURE 2. *End points of the whole-brain fibers.* **A**, *oblique view.* **B**, *close-up view of the superior bihemispheric surface. The yellow star shows the location of the precentral gyrus (motor strip) in* **A** *and* **B**. *Note the clear distinction of gyri and sulci such as the interhemispheric fissure; precentral and postcentral gyrus; superior and middle frontal gyrus; and central, precentral, postcentral, superior frontal, and intraparietal sulcus. End points are color coded by direction.*

planning of brain lesions, aiming to show the increased accuracy obtained and the clinical implication of the findings.

PATIENTS AND METHODS

HDFT Technique

Six neurologically healthy adults (5 male; all right handed; age range, 22-31 years) from the local University of Pittsburgh community took part in this experiment, conducted as part of a larger data collection effort associated with the 2009 Pittsburgh Brain Competition. Thirty-six patients with brain lesions were studied. To simplify the analysis, we have grouped the studied cases into 3 major types of intracerebral lesions: high-grade gliomas (including World Health Organization grades 3 and 4), low-grade gliomas (grades 1 and 2), and cavernomas. Other types of lesions were excluded from analysis (Table 1). Normal subjects and patients were prescreened before scanning to rule out any contra-indications to magnetic resonance (MR) imaging (MRI). The internal review board at the University of Pittsburgh approved all of the procedures used here, and written consent was obtained from all participants before testing.

Image Acquisition and Reconstruction

DSI data were acquired on a 3-T Tim Trio System (Siemens) using a 32-channel coil. A novel head stabilizer device was used to prevent head motion. This custom-built plastic device is locked to the Siemens 32-channel coil and has an adjustable restraint piece that rests against the bridge of the nose. The height and angle of this interface against the bridge of the nose are adjusted to each patient's comfort level. Once locked, it stabilizes the head against the coil itself to minimize motion during the scan. The study involved a 43-minute, 257-direction scan with a twice-refocused spin-echo echo planar imaging sequence and multiple b values (repetition time = 9916 milliseconds, echo time = 157 milliseconds, voxel size = 2.4 × 2.4 × 2.4 mm, field of view = 231×231 mm, bmax = 7000 s/mm^2, bmin = 500 s/mm^2). For anatomical comparisons, we also included high-resolution anatomical imaging using a 9-minute T1-weighted axial magnetization-prepared rapid-acquisition gradient-echo sequence (repetition time = 2110 milliseconds, echo time = 2.63 milliseconds, flip angle = 8°, number of slices = 176, field of view = 256 × 256 mm^2, voxel size = 0.5 × 0.5 × 1.0 mm^3). DSI data were reconstructed with a generalized Q-ball imaging approach.[25] The orientation distribution functions were reconstructed to 362 discrete sampling directions for each pixel and with a diffusion distance scaling parameter of 0.5 to 1.2. This means that the resulting reconstructed orientation distribution function can cover 0.5 to 1.2 SDs of the free water diffusion distance in the underlying voxel (measured in micrometers).[25]

Fiber Tracking and Analysis

For the HDFT data sets, all fiber tracking was performed with DSI-Studio.[26] We adopted a whole-brain fiber tracking procedure and an orientation distribution function–streamlined region of interest–based approach.[25] Tracts were generated with the use of an orientation distribution function–streamlined version of the Fiber Assignment by Continuous Tracking algorithm.[2,28-30,32] Using a random seeding approach, we initiated tracking, from each random position within the seed mask, in the direction of the most prominent fiber. Fiber progression continued with a step size of 0.5 to 1.2 mm, minimum fiber length of 0 to 20 mm, and turning angle threshold of 60°. To smooth each track, the next directional estimate of each voxel was weighted by 20% of the previous moving direction and 80% by the incoming direction of the fiber. The tracking was terminated when the relative fractional anisotropy for the incoming direction dropped below a preset threshold (0.03-0.06, depending on the subject) or exceeded a turning angle of 60°. The fractional anisotropy termination threshold was adjusted on a per-subject basis, depending on the relative signal-to-noise ratio of each scan.[28] This is critical for single-subject–based tractography studies in which individual differences in signal-to-noise ratio can vary across subjects and scan sessions. Identifying optimal tracking parameters that maximize both within-subject and across-scan reliability is a focus of future studies and well beyond the scope of this project. Once tracked, all streamlines were saved in the TrackVis file format. Segmentation of the fiber tracts was performed with TrackVis software.[33]

Fiber Dissection Technique

Twenty normal brains were obtained at routine autopsy. The specimens were fixed in a 10% formalin aqueous solution for at least 4 weeks

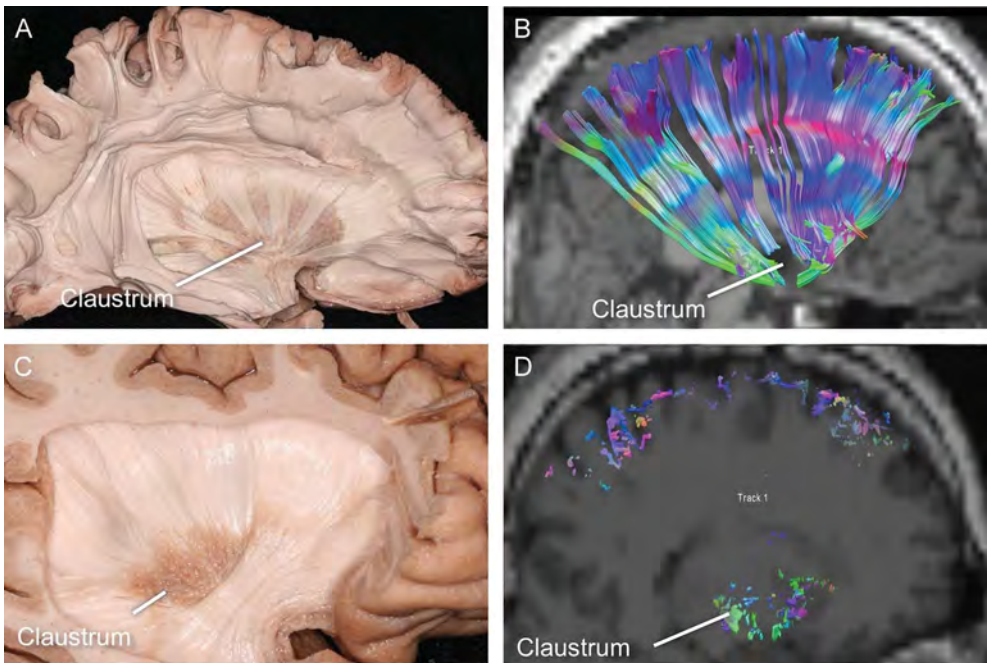

FIGURE 3. *Claustrocortical projection system.* **A**, *lateral view, right hemisphere. Fiber dissection has been performed to expose the claustrocortical fibers (dorsal external capsule).* **B**, *high-definition fiber tractography of the claustrocortical fibers.* **C**, *lateral and close-up view of the claustrocortical fibers in an anatomical specimen.* **D**, *end points of the claustrocortical fibers resembling the ovoid shape of the claustrum and its cortical termination fields.*

and then were subsequently frozen for 2 additional weeks at −16°C, according to the method introduced by Klinger and coworkers.[6,34] Progressive dissection of the white matter tracts was performed by peeling off the gray matter and isolating the fiber bundles in their glial sheets. We undertook the fiber dissection studies at the Microneurosurgical Anatomy Laboratory at the University of Florida and at the Surgical Neuroanatomy Laboratory at University of Pittsburgh, with the aid of microsurgical instrumentation, surgical microscope (6-40 magnification; Carl Zeiss, OPMI CS-NC), and high-definition exoscope (Karl Storz, Hopkins II). Microdissection studies were used for comparison with fiber tracking results.

RESULTS

HDFT in the Normal Brain

We analyzed and categorized our results on the basis of selected anatomical features that are unique and typical of the normal human brain and that, to the best of our knowledge, have not been successfully replicated with current fiber tracking techniques. These results are not intended to be a comprehensive study of major fiber tracts but rather a selective study of distinct neuroanatomical features that have been challenging to replicate (Table 2).

Cortical Termination of the Fibers

The fiber reconstruction of the whole brain (average, 250 000 streamlines) shows with extraordinary precision the termination of the fibers in the cortical surface. The fibers fill up most gyri and leave the gap for the sulci, resembling normal cortical anatomy. Most gyri and sulci are easily recognized solely on the basis of the end points of the fiber tracts, which firmly replicate the intricate pattern of cortical folding. The similarity with structural MR sequences and with anatomical specimens is striking (Figures 1 and 2).

Subcortical Termination of the Fibers

Many cortical projection fibers end at or originate from defined subcortical structures. We illustrate here the precision of HDFT with the case of the claustrocortical fibers.

Claustrocortical Projection System. The claustrum is a thin grey nucleus located deep to the insular cortex with unknown functional significance. Crick and Koch[35] recently discussed the role of the claustrum on consciousness. Histological studies in animals have revealed the existence of a network of connections between the claustrum and the cortex, and recent studies combining anatomical fiber dissection and DTI have supported the presence of a claustrocortical projection system in the human brain.[36] In our previous studies using DTI, the fibers of the dorsal external capsule appear to converge in the claustrum. Given the lack of precision of DTI, these fibers, instead of ending in the claustrum, formed a continuous loop ("false continuation") of fibers running from the claustrum

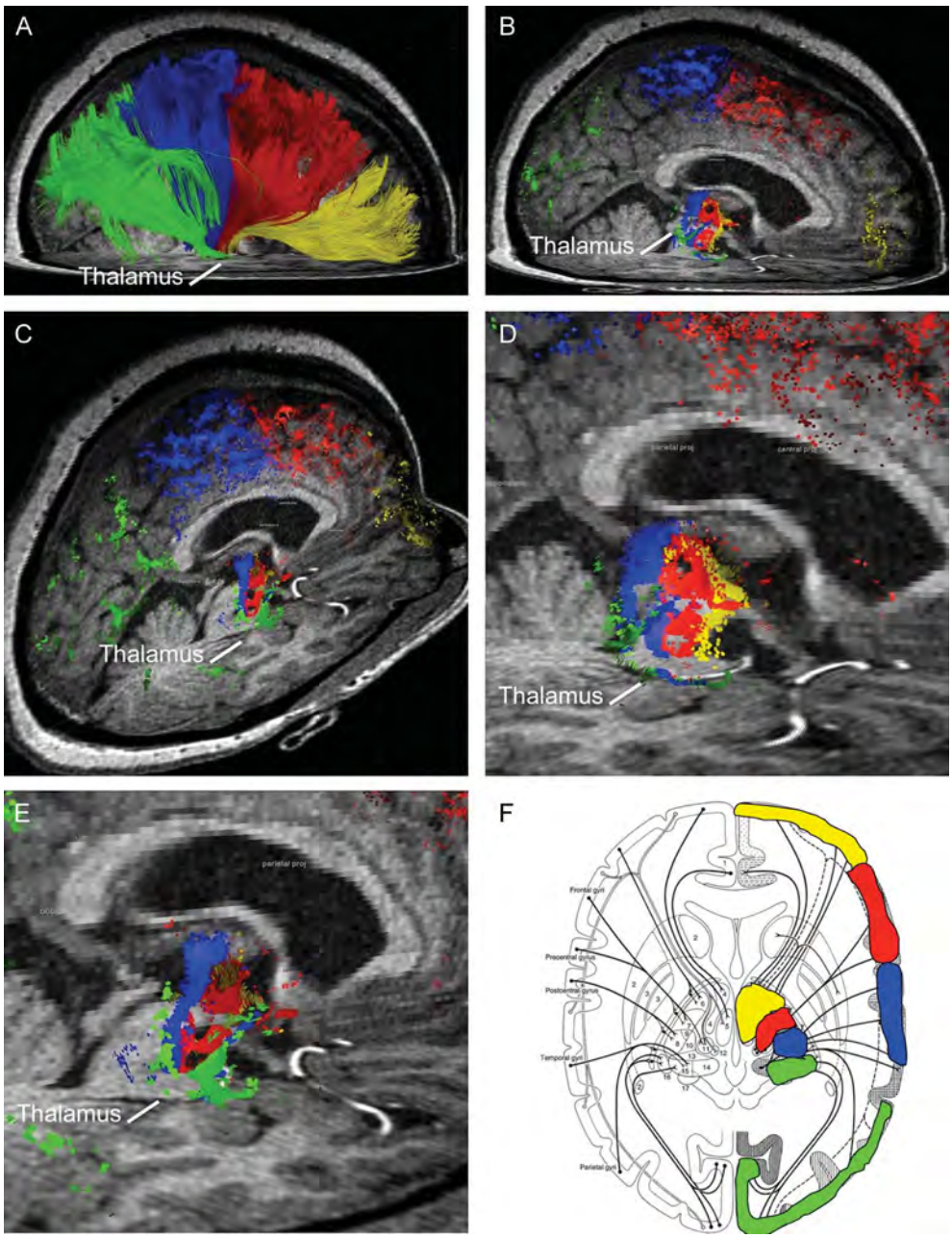

FIGURE 4. *Thalamocortical projection system.* **A**, *high-definition fiber tractography (HDFT) of the right thalamic radiations. Color coding: yellow, prefrontal; red, precentral-premotor; blue, postcentral-precuneus; green, parieto-occipital.* **B** *through* **E**, *end points of the right thalamic radiations. Note the segmentation of the thalamus based on the termination of the fibers.* **B**, *lateral view.* **C**, *posterolateral view.* **D**, *lateral and close-up view.* **E**, *posterolateral and close-up view.* **F**, *schematic diagram of the thalamic radiations based on neurohistological studies (from Nieuwenhuis et al[37]). Note the precise matching between neurohistological studies and HDFT.*

region to the cortex. HDFT shows with remarkable precision the anatomy of the claustrocortical projections, including the sharp termination of the fibers in the claustrum and the cortex. It is important to consider that this group of long projection fibers that forms the dorsal external capsule is one of the thinnest projection systems in the human brain. The dot cloud formed by the end points of the fibers at the claustrum resembles the thin and ovoid shape of this enigmatic

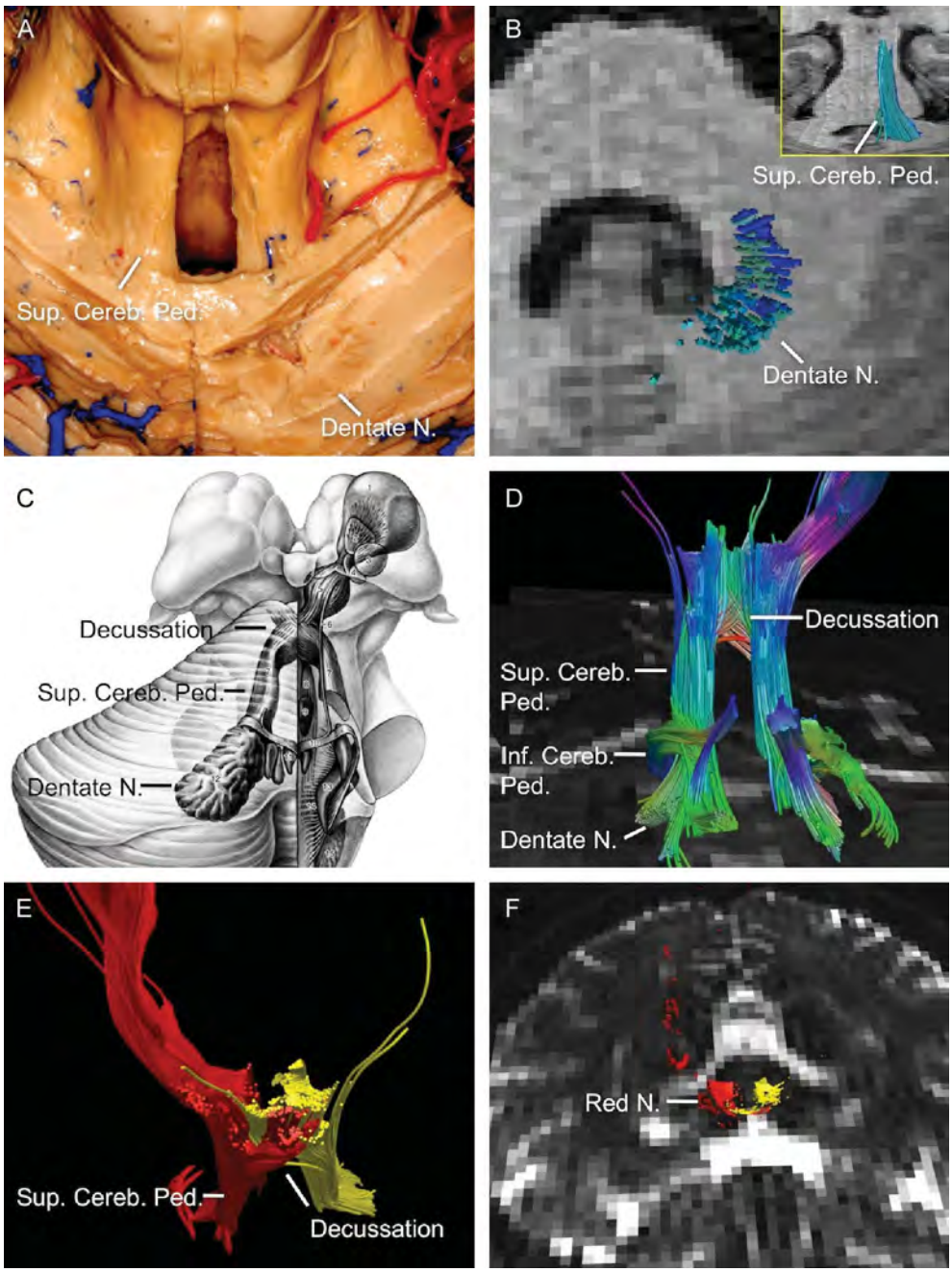

FIGURE 5. *Superior cerebellar peduncles.* **A**, *anatomical dissection, posterior view. The quadrangular lobule of the cerebellum has been removed to expose the superior cerebellar peduncles (Sup. Cereb. Ped.) and right dentate nucleus.* **B**, *high-definition fiber tractography (HDFT) of the right superior cerebellar peduncle (inset); the fibers arise precisely from the dentate nucleus (N.).* **C**, *posterior view; artistic drawing of the superior cerebellar peduncles showing the origin of the fibers at the dentate nucleus and the decussation of the fibers before the level of the red nuclei (from Nieuwenhuis et al[37]).* **D**, *posterior view; HDFT of bilateral superior and inferior cerebellar peduncles displaying the same anatomy as in* **C**. **E**, *anterior view. The right superior cerebellar peduncle is red and the left is yellow. Note the decussation of the fibers.* **F**, *end points of the superior cerebellar peduncles replicating the round shape of the red nuclei.*

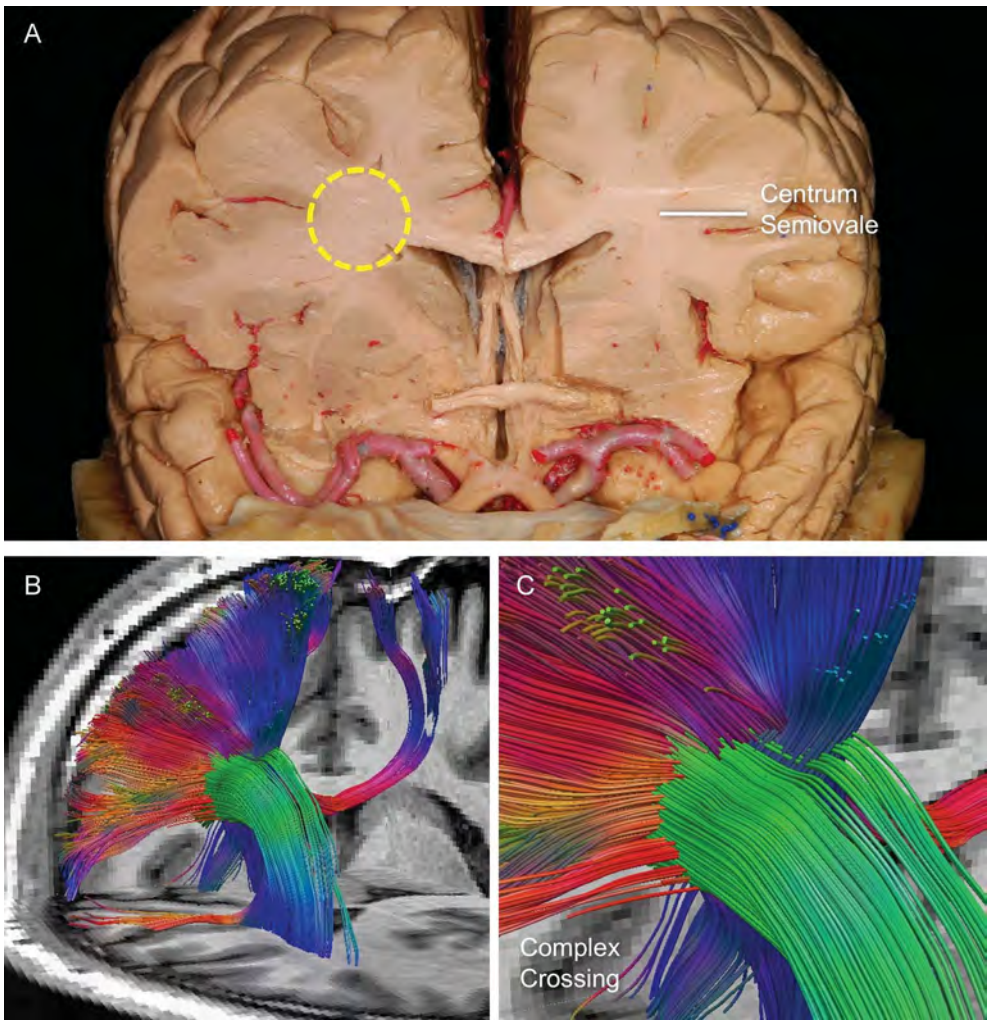

FIGURE 6. *Centrum semiovale.* **A**, *anatomical specimen, anterior view. A coronal cut has been performed at the level of the anterior commissure to expose the white matter that corresponds to the centrum semiovale.* **B**, *high-definition fiber tractography at the level of the centrum semiovale revealing the complex architecture of this white matter region. The fibers are color coded for transverse (red), longitudinal (green), and vertical (blue) directions. Note the ability to reconstruct multiple crossing of fibers and to follow the fibers through the complex crossing.* **C**, *close-up view of* **B**.

subcortical structure compared with human brain anatomical specimens (Figure 3).

Subcortical Termination and Subcortical Fiber-Based Segmentation

As we have previously stated, the end points of the fibers resemble cortical and subcortical structures. Here, we will show that HDFT can also provide segmentation of subcortical structures based on their pattern of structural connectivity.

Thalamocortical Projection System. The thalamic radiations or peduncles are well described in classic neuroanatomy texts.[37] Previous authors have identified specific connections between human thalamus and cortex using a probabilistic tractography algorithm with diffusion imaging data.[38] Here, we use a deterministic approach, HDFT, to depict with precision the thalamic radiating fibers from/to the frontal, central, parietal, and occipital regions. The compelling aspect is that HDFT not only shows the precise origin/termination of the thalamocortical fibers but also presents a structural organization of the thalamus based on the origin/termination of the fibers that is in agreement with neurohistological studies. Analyzing the end points of the radiating fibers, we find that fibers from the orbitofrontal region are linked to the most medial and anterior portion of the thalamus (dorsal medial zone); fibers from the prefrontal area

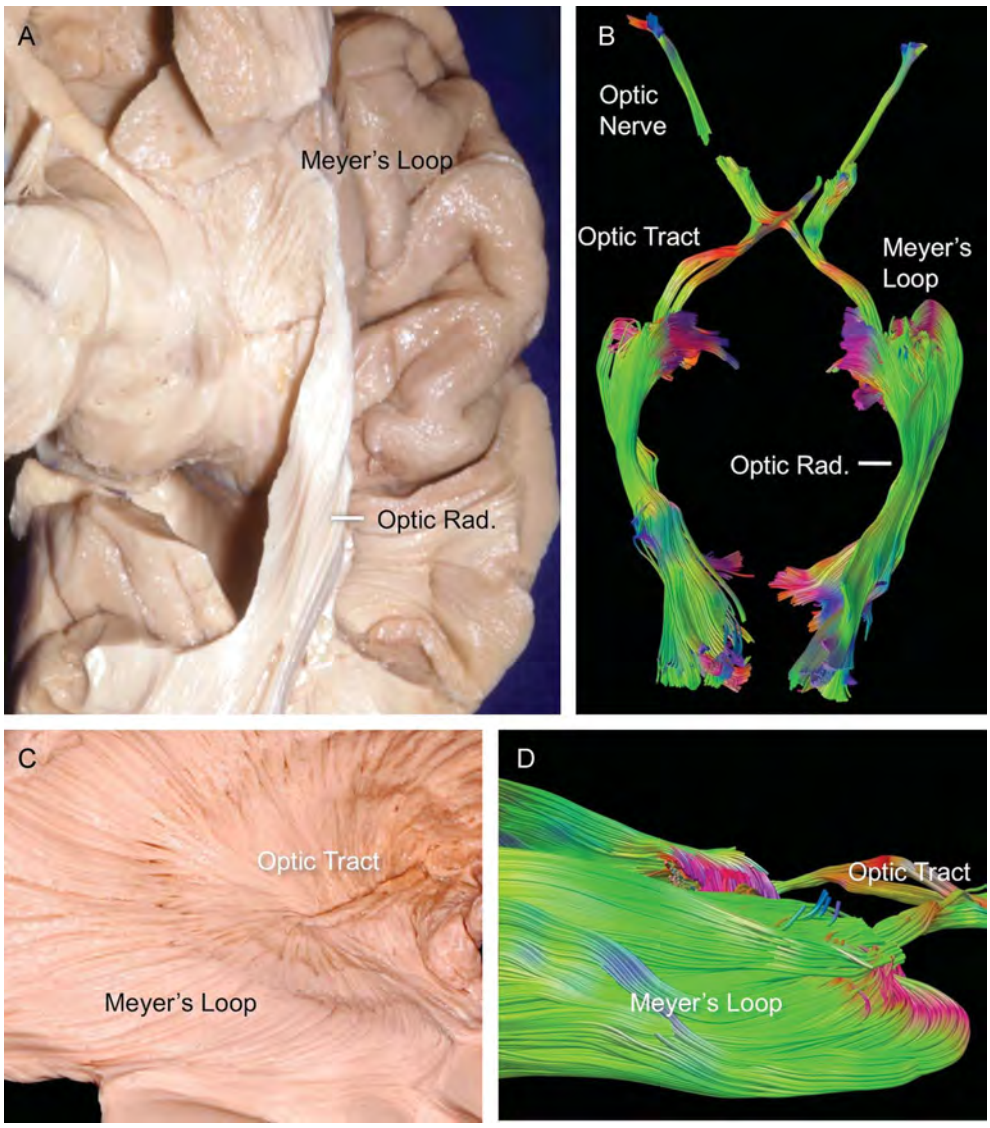

FIGURE 7. *Visual pathways.* **A**, *fiber dissection of the visual pathways, left hemisphere, basal view.* **B**, *high-definition fiber tractography (HDFT) of the visual pathways.* **C**, *close-up and lateral view of the right Meyer loop as exposed with fiber dissection.* **D**, *HDFT of the right Meyer loop to correlate with* **C**.

arise or terminate in the ventral anterior and lateral zone of the thalamus; central lobule fibers project in the thalamus just posterior to the prefrontal projection zone (ventral posterior zone); and parieto-occipital fibers project to the most posterior and inferior regions of the thalamus (pulvinar and lateral geniculate body; Figure 4).

Double Subcortical Termination and Decussation of Fibers: The Superior Cerebellar Peduncle

The main efferent pathway of the cerebellum is the superior cerebellar peduncle. It is well established that fibers from the deep cerebellar nuclei (dentate, emboliform, and globose nuclei) project to the contralateral red nucleus via the superior cerebellar peduncle. Importantly, before reaching the ipsilateral red nucleus (located in the upper midbrain), some of the fibers of the peduncle cross the midline (decussation) at the lower midbrain to reach the contralateral red nucleus. Some fibers travel directly to the thalamus without crossing at the midbrain or stopping at the red nucleus. Our HDFT-based studies show the origin of the fibers in the dentate nucleus, their termination in the ipsilateral red nucleus and thalamus, and the decussation of some fibers at the lower midbrain to

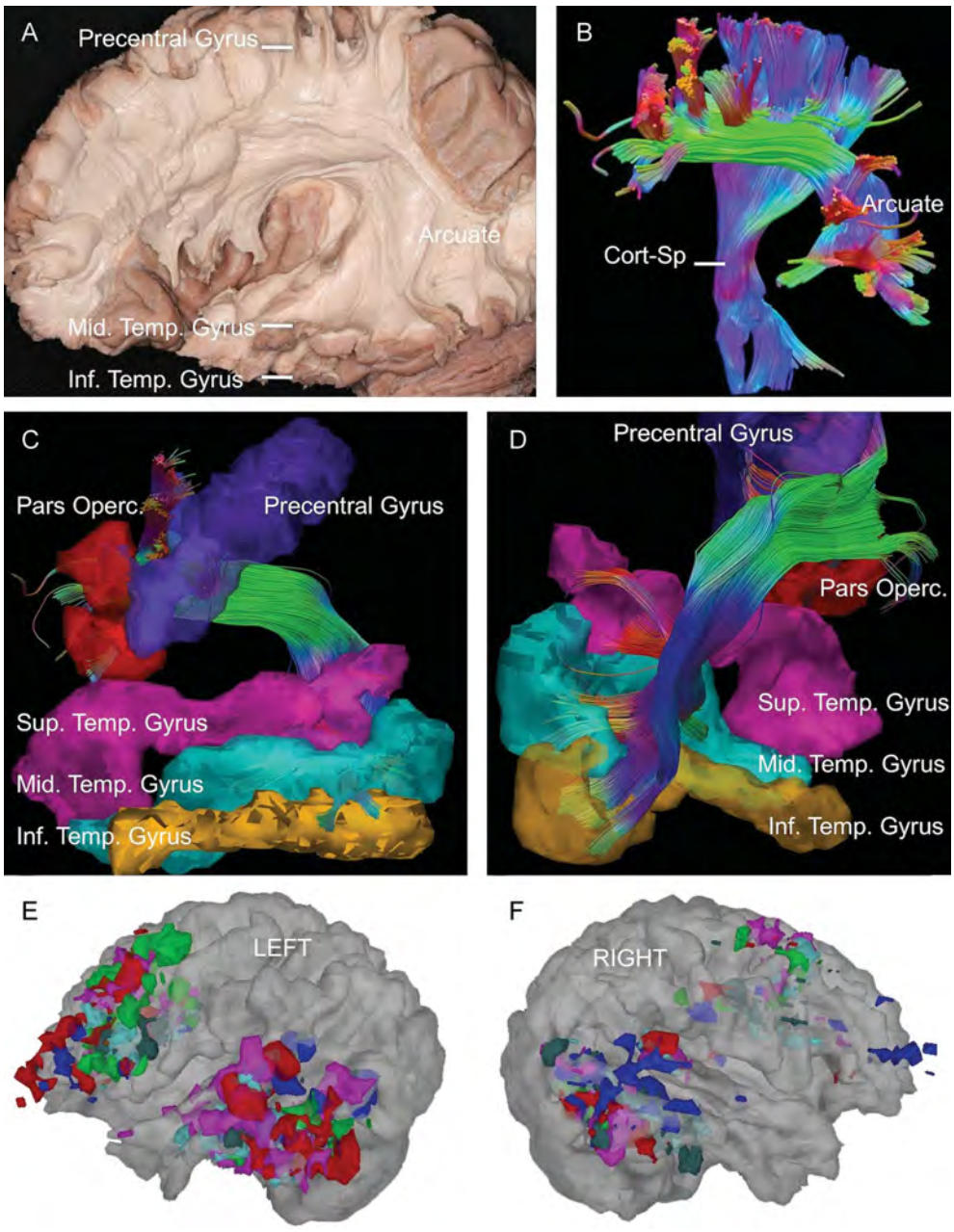

FIGURE 8. *Arcuate fascicle.* **A**, *fiber dissection of the arcuate fascicle, left hemisphere.* **B**, *high-definition fiber tractography (HDFT) of the arcuate and corticospinal (Cort-Sp) tracts to correlate with* **A**. **C**, *terminal branches of the arcuate fascicle as studied with HDFT.* **D**, *same as* **C**, *posterior view.* **E**, *summary of the cortical terminations of the arcuate fascicle in the left hemisphere.* **F**, *same as* **E** *but right hemisphere. Each color represents a single subject. Six subjects were studied (red, dark blue, light blue, pink, purple, dark green, light green). Colors (end points) are superimposed in certain regions for some subjects. Note the decreased density of terminal fibers in the right frontal opercular (Operc.) region (Broca area in the left side) and posterior temporal (Temp.) region compared with the left hemisphere. Inf., inferior; Mid., middle; Sup., superior.*

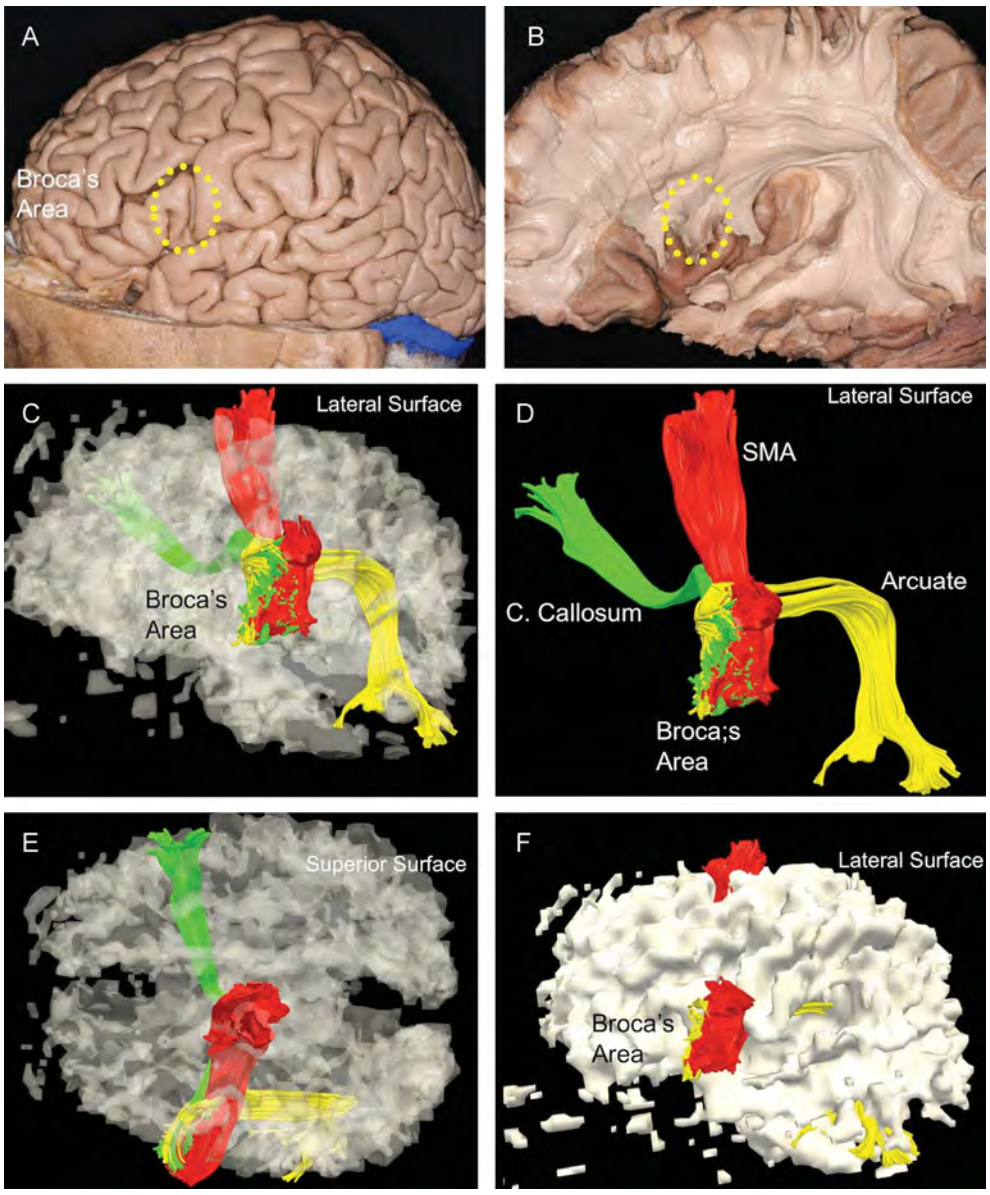

FIGURE 9. *Connectivity of the Broca area.* **A**, *left hemisphere; the yellow interrupted circle shows the location of the dorsal Broca area (pars opercularis).* **B**, *fiber dissection of the left arcuate tract; the yellow interrupted circle shows the fibers arising from the Broca area.* **C** *and* **D**, *high-definition fiber tractography of the Broca area, lateral view. There are 3 distinct tracts connecting with the Broca area: arcuate (yellow), commissural fibers of the corpus (C.) callosum (green), and association fibers to the ipsilateral supplementary motor area (SMA; red).* **E**, *same as in* **C** *and* **D** *but superior view.* **F**, *same as* **C** *and* **D,** *but the commissural fibers have been excluded to show the segmentation of fibers within the Broca area.*

reach the contralateral red nucleus. The dot cloud formed by the end points of the fibers at the cerebellum and mesencephalon accurately matches the peculiar semimoon shape of the dentate nucleus and the round shape of the red nuclei, respectively (Figure 5).

Triple Crossing: The Centrum Semiovale

The centrum semiovale is defined as the common central mass of white matter with an oval appearance in horizontal sections of the brain just above the level of the lateral ventricles. Previous anatomical and DTI studies have shown that this is a highly

TABLE 3. High-Definition Fiber Tractography for Brain Lesions

Type of Lesion	Findings	Figure
High-grade glioma	Lack of fibers within tumor necrosis	10-12
	Fiber disruption coincidental with necrosis	
	Fiber displacement related to mass effect	
	Quantitative analysis of the structural impact of the tumor in the fiber tracts	
Low-grade glioma	Focal gliomas: lack of fibers within the main core of the tumor	13-15
	Diffuse gliomas: trapped fibers within tumor	
	Absence of fiber disruption	
	Fiber tracts displaced and located at the tumor–white matter interface	
Cavernoma	Lack of fibers within cavernoma	15-20
	Combination of fiber disruption and displacement depending upon frequency and severity of hemorrhagic events	
	Accurate replication of brainstem corticectomy	

complex region of the white matter composed from lateral to medial by the arcuate and superior longitudinal fascicles (anteroposterior orientation), corona radiata (craniocaudal orientation), and corpus callosum fibers (mediolateral orientation).[6] At the centrum semiovale, these groups of fibers cross each other in the 3 spatial planes. This triple or complex crossing of fibers severely limits fiber tracking techniques such as DTI. Our HDFT studies have shown a superior ability to solve the crossing problem; this is particularly illustrated in the region of the centrum semiovale. With HDFT, we are able to follow the radiating fibers of the corpus callosum as they cross, from medial to lateral, the vertical fibers of the coronal radiata and the horizontal fibers of the arcuate and superior longitudinal fascicles. Similarly, the fibers of the corona radiata and arcuate/superior longitudinal fascicles can be followed through these complex crossings without missing any significant volume of fibers (Figure 6).

Complex Angulations: The Meyer Loop

The fibers of the anterior part of the optic radiations or the Meyer loop travel anteriorly and laterally from the lateral geniculate body to reach the anterior edge of the roof of the temporal horn, where they curve posteriorly to join the middle and posterior part of the optic radiations in their path toward the calcarine cortex.[39] The pronounced curvature of Meyer loop fibers is a challenge for fiber tracking methods. HDFT shows Meyer loop fibers arising from the lateral geniculate body and replicates the complex angulation successfully (Figure 7).

Arborization of Terminal Fibers and Multiple Cortical Terminations: The Inside-out Approach

The arcuate fascicle is described as a reversed C-shaped structure that surrounds the insula and interconnects the frontal and temporal lobes. Fiber dissection and fiber tracking studies have investigated the cortical areas interconnected by the arcuate fascicle.[6,40-42] Given their technical constraints, these attempts have provided an approximation or estimation of interconnected cortical regions that are largely based on preexisting anatomical knowledge rather than direct visualization.[43] Using HDFT, we are able to visualize the different branches of the arcuate fascicle at the frontal and temporal regions. These terminal branches can be followed into their particular gyri/sulci of origin or destiny. Furthermore, fibers of the arcuate fascicle can be tracked from 1 concrete gyrus in the frontal region such as the pars opercularis to its temporal counterpart such as the posterior segment of the inferior temporal sulcus and middle temporal gyrus. The superposition of segmented cortical areas facilitates the analysis of the pattern of cortical terminations of the arcuate fascicle, revealing a much more complex and rich scheme than previously stated and confirming the laterality of the arcuate tract and its relation to language function. HDFT allows an inside-out approach to structural brain connectivity: from the main stem of the fiber tract to the cortical termination (Figure 8).

Cortical Connectivity and Segmentation: The Outside-in Approach

An alternative way of looking at structural brain connectivity is the outside-in approach: from cortical region to fiber tracts. Magnetoencephalography, resting-state MR studies, and probabilistic tractography methods have all provided new insights into brain connectivity in between cortical regions, but they cannot inform about the actual fiber pathways that interconnect those regions. HDFT, however, may allow direct visualization of structural pathways that interconnect distant cortical regions. Depending on the cortical regions of interest, HDFT may show several modalities of fibers arising from or terminating in that same location. As an illustration, our studies on cortical connectivity revealed that pars opercularis (dorsal Broca area or Brodmann area 44) contributed fibers to 3 distinct pathways: arcuate fascicle (pars opercularis to posterior middle temporal gyrus), corpus callosum (pars opercularis to contralateral middle frontal gyrus or dorsolateral prefrontal cortex), and short association fascicle to

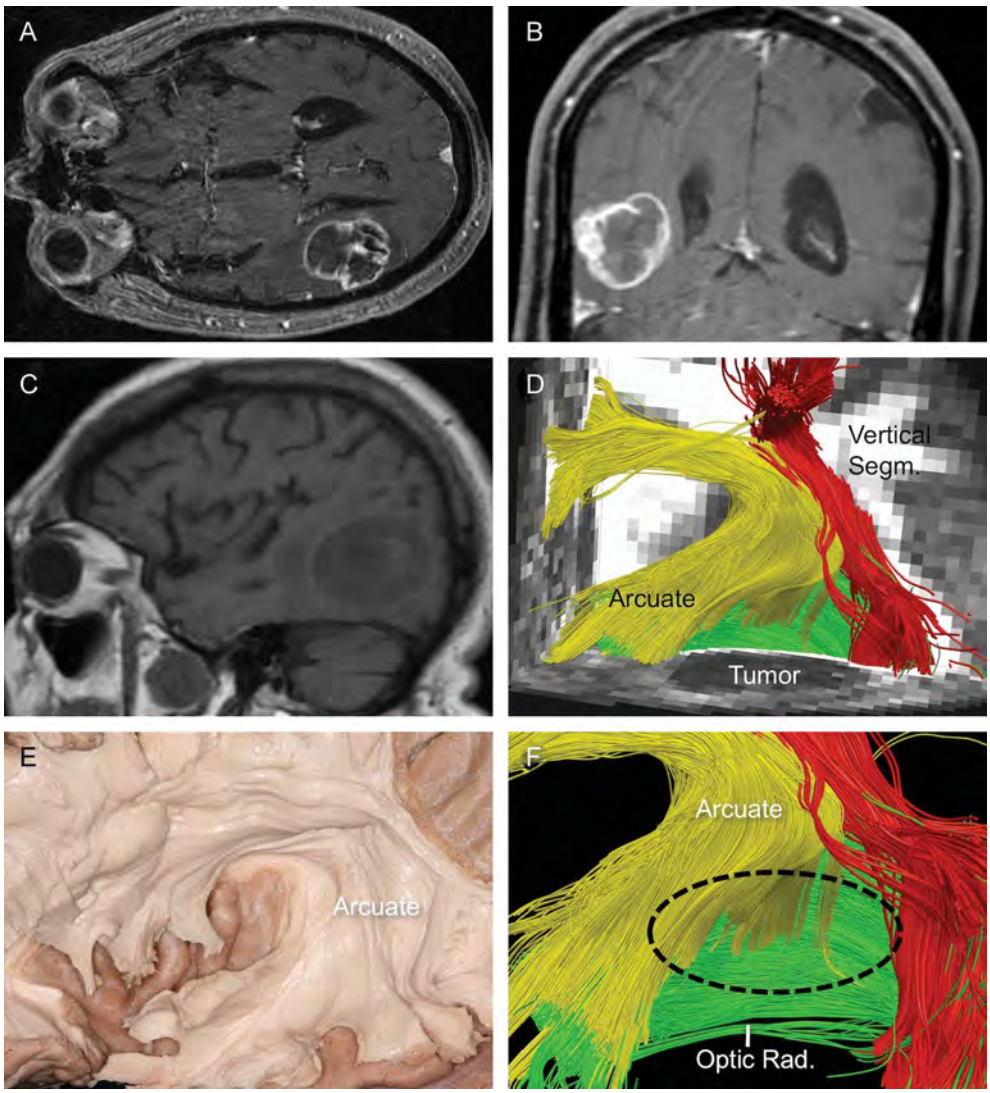

FIGURE 10. *Illustrative case 1. Left posterior temporal high-grade glioma.* **A** *through* **C**, *structural magnetic resonance imaging (axial, coronal, and sagittal, respectively; the scans have been flipped to facilitate correlation with* **D**-**F**). **D**, *high-definition fiber tractography showing the displacement and disruption of the arcuate fascicle (yellow).* **E**, *fiber dissection of the left arcuate tract to correlate with* **D** *and* **F**. **F**, *close-up view of the disruption of the temporal branch of the arcuate tract caused by the tumor. Note that the optic radiations (Rad.) are pushed medially but are preserved.*

ipsilateral supplementary motor area or posterior superior frontal gyrus. Interestingly, association fibers to the temporal lobe via the arcuate fascicle are located more posteriorly in pars opercularis, whereas association fibers to the frontal lobe are situated more anteriorly and commissural fibers to the contralateral frontal region are homogeneously distributed (Figure 9).

HDFT for Brain Lesions

Here, we describe our most significant findings when applying HDFT for the presurgical study of 3 types of intracerebral lesions: high-grade gliomas, low-grade gliomas, and cavernomas (Table 3). It is critical to point out that the application of HDFT in this study was not intended to modify or influence the clinical decision-making process but rather to analyze post hoc the potential clinical implications of the findings.

High-Grade Gliomas

These lesions are typically characterized by necrosis and surrounding edema. HDFT is able to show with precision the disruption caused by the necrotic lesion and rapid tumor growth

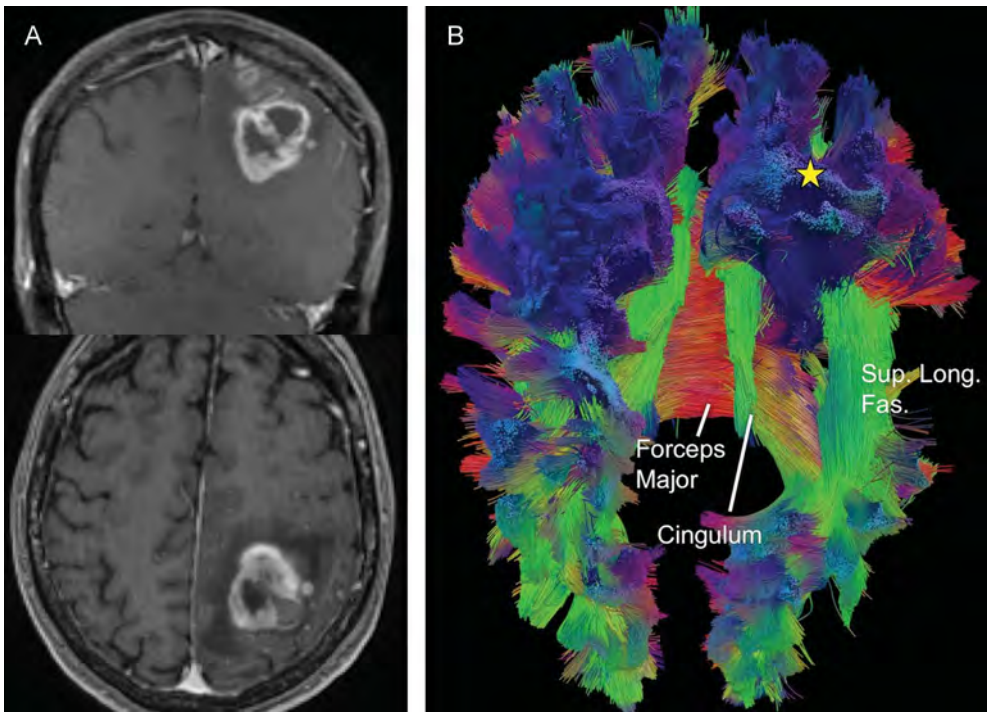

FIGURE 11. *Illustrative case 2. Left superior parietal lobule high-grade glioma.* **A**, *structural magnetic resonance image (coronal, axial).* **B**, *high-definition fiber tractography showing anterior displacement of the postcentral gyrus, disruption of the forceps major and cingulum, and displacement of the superior longitudinal fascicle (Sup. Long. Fas.).*

and differentiate this from the displacement caused by regional mass effect. No fibers are found within the tumor tissue. Importantly, HDFT can provide detailed qualitative and quantitative analyses of the structural impact of the tumor in the fiber tracts. From the qualitative point of view, we can perform a separate analysis of defined fiber tracts and identify whether there is total disruption, partial disruption, or just displacement of the tract. From the quantitative point of view, we can determine the number of streamlines (a relative measurement of number of axonal fibers) and the volume of a fiber tract and compare these results with the contralateral counterpart (intrasubject comparison) or with a normal-subject fiber tract database (intersubject comparison). As a consequence, beyond discerning the location of eloquent fiber tracts in relation to the tumor as done by current fiber tracking techniques, we can obtain a detailed analysis of the structural impact of the tumor that may influence the surgical decision-making process and may carry prognostic value.

ILLUSTRATIVE CASES

Case 1

A 76-year-old right-handed man presented with speech disturbances of sensitive predominance (anomia, paraphasias). An MRI study showed a lesion compatible with a high-grade glioma situated in the posterior part of the left temporal lobe. We completed an HDFT study and segmented the fiber tracts surrounding the tumor. We did not see any fibers within the necrotic and enhancing part of the tumor. The temporal part of the arcuate fascicle was displaced forward and upward; we identified partial disruption of fibers at the posterior part of the tract, presumably affecting the fibers that connect with the Wernicke area. The vertical or parietotemporal segment of the arcuate fascicle[6] was mildly displaced backward with no apparent disruption. The optic radiations were significantly displaced medially with no obvious disruption (Figure 10).

Case 2

A 58-year-old woman presented with headache and intermittent paresthesias in the right upper extremity. An MRI study revealed the presence of a contrast-enhanced intracerebral lesion suggestive of high-grade glioma located at the superior parietal lobule with necrosis and surrounding edema. A presurgical HDFT study revealed the following: No fibers were shown within the necrotic or enhancing part of the tumor; the precentral and postcentral gyri were easily identified on the basis of the fibers that filled up the gyri; the precentral gyrus had a normal appearance, and even the Ω sign for the hand motor area was noted; the postcentral gyrus fibers

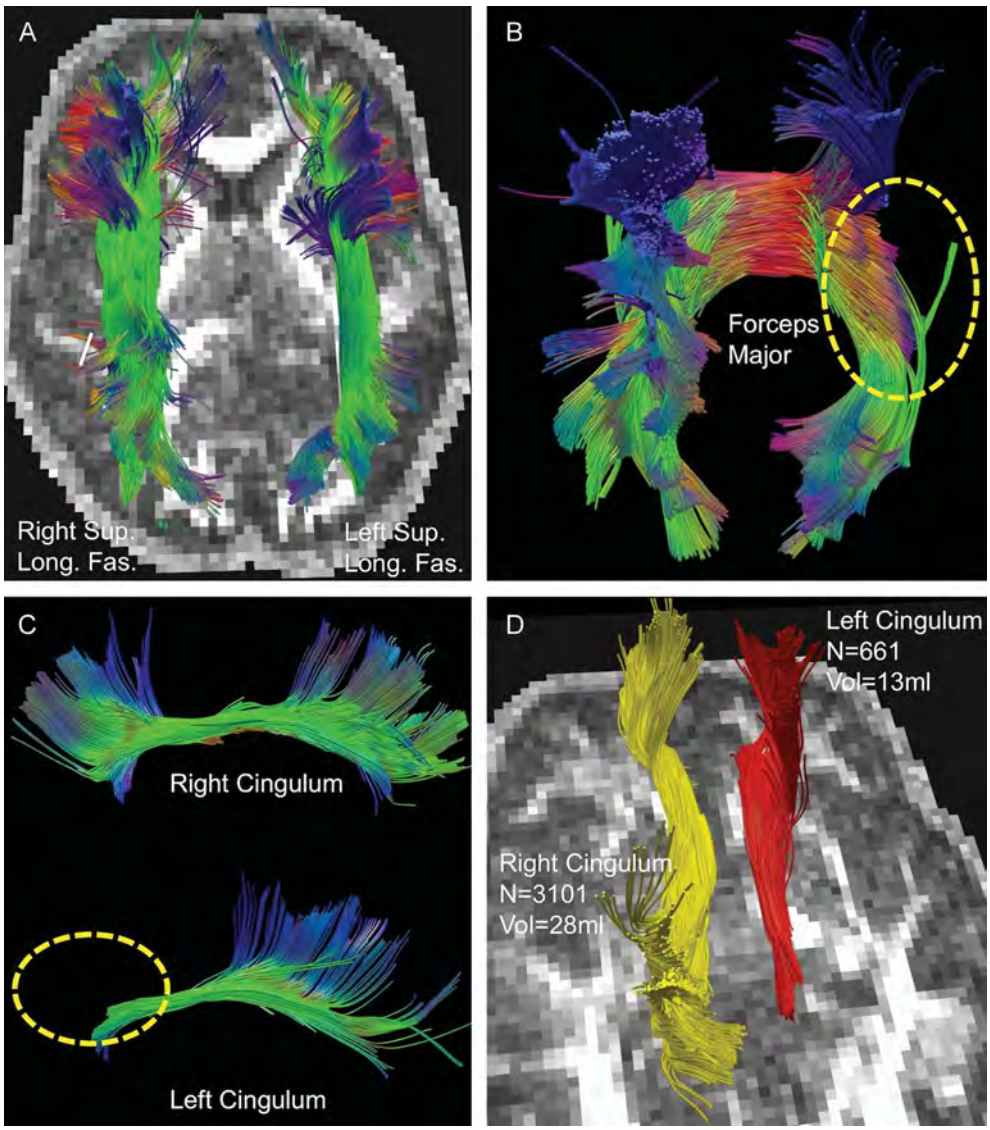

FIGURE 12. *Illustrative case 2 (continuation). Qualitative and quantitative study of the impact of the tumor on related fiber tracts.* **A**, *superior longitudinal fascicles (Sup. Long. Fas.).* **B**, *forceps major.* **C**, *cinguli.* **D**, *quantitative comparison of the cinguli.*

were displaced forward, and no fibers were identified posterior to this gyrus (Figure 11); the left superior longitudinal fascicle, in comparison with the contralateral superior longitudinal fascicle, appeared to be thinner as a consequence of mass effect and compression; the left wing of the forceps major (splenial commissural fibers) was severely disrupted by the tumor necrosis, causing a partial disconnection between the parieto-occipital cortices; and finally, the well-known connection of the left cingulum with the precuneus[6] was completely disrupted by the tumor. A quantitative analysis of the cinguli showed that the left cingulum had an $>$ 75% decrease in the relative number of fibers and an almost 50% decrease in the volume of the tract (left cingulum: 661 streamlines, 13 mL; right cingulum: 3101 streamlines, 28 mL; Figure 12).

Low-Grade Gliomas

Major dilemmas when dealing with low-grade gliomas are whether there are any fibers (particularly functional fibers) within the tumor and what the architecture and function are of the white matter that surrounds the tumor.[44-48] Our preliminary experience suggests that HDFT may provide unique insights into these questions. Grossly, low-grade gliomas can be classified as focal when they grow within a single gyrus or diffuse when they affect several gyri and sulci.[48] In the focal gliomas from our limited

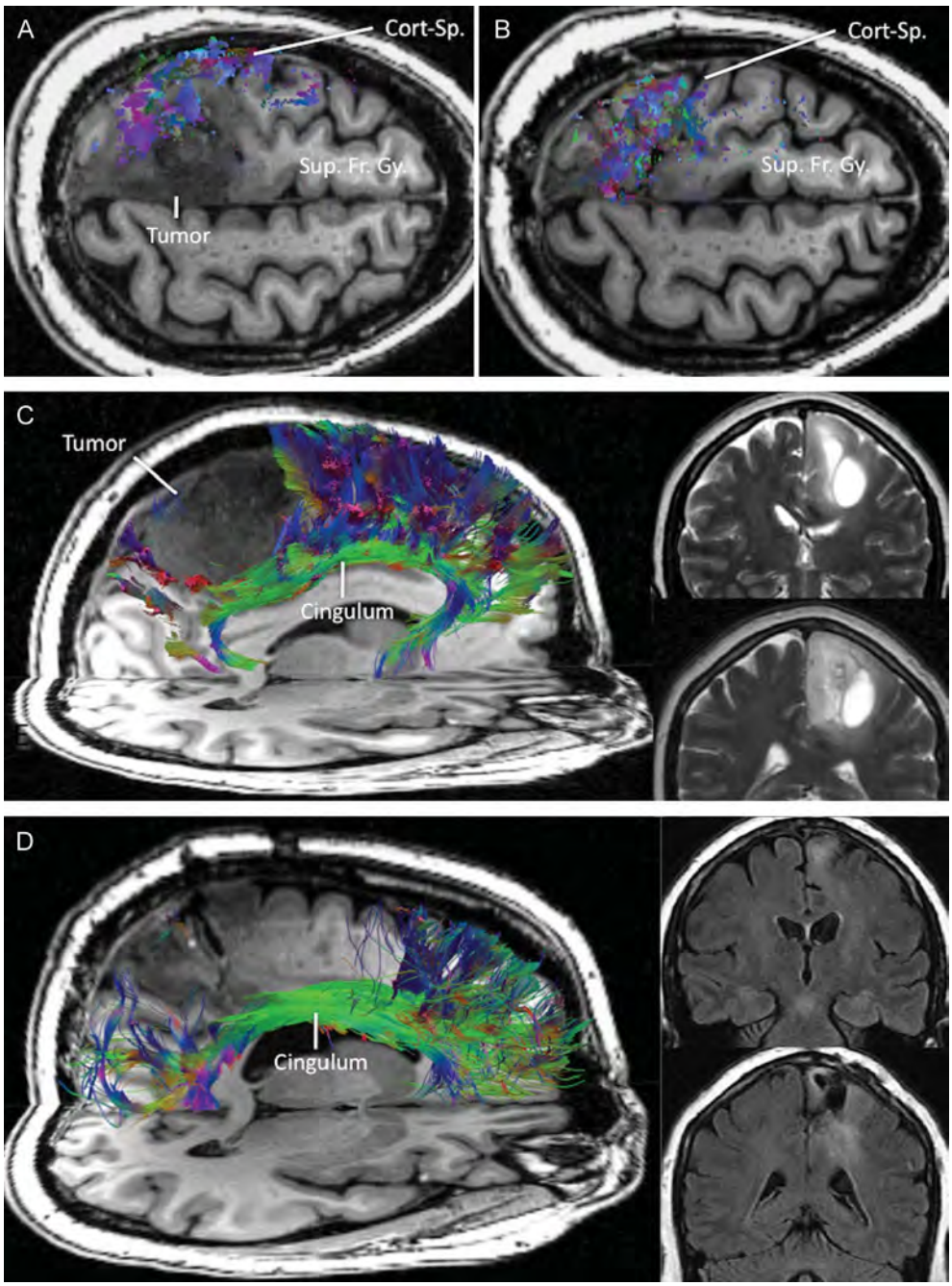

FIGURE 13. *Illustrative case 3. Supplementary motor area low-grade glioma.* **A**, *preoperative high-definition fiber tractography (HDFT) study showing the cortical end points of the left corticospinal (Cort-Sp) tract (axial slice has been rotated to facilitate comparison with* **C** *and* **D**). **B**, *3-month postoperative HDFT study; the corticospinal tract end points have shifted to their normal position in the precentral gyrus.* **C**, *preoperative HDFT study and coronal T2-weighted slices; the main stem of the cingulum has been displaced downward.* **D**, *postoperative HDFT study and coronal fluid-attenuated inversion-recovery slices; the mass effect on the main stem of the cingulum has disappeared; the fluid-attenuated inversion-recovery sequences evidence residual tumor. Sup. Fr. Gy., superior frontal gyrus.*

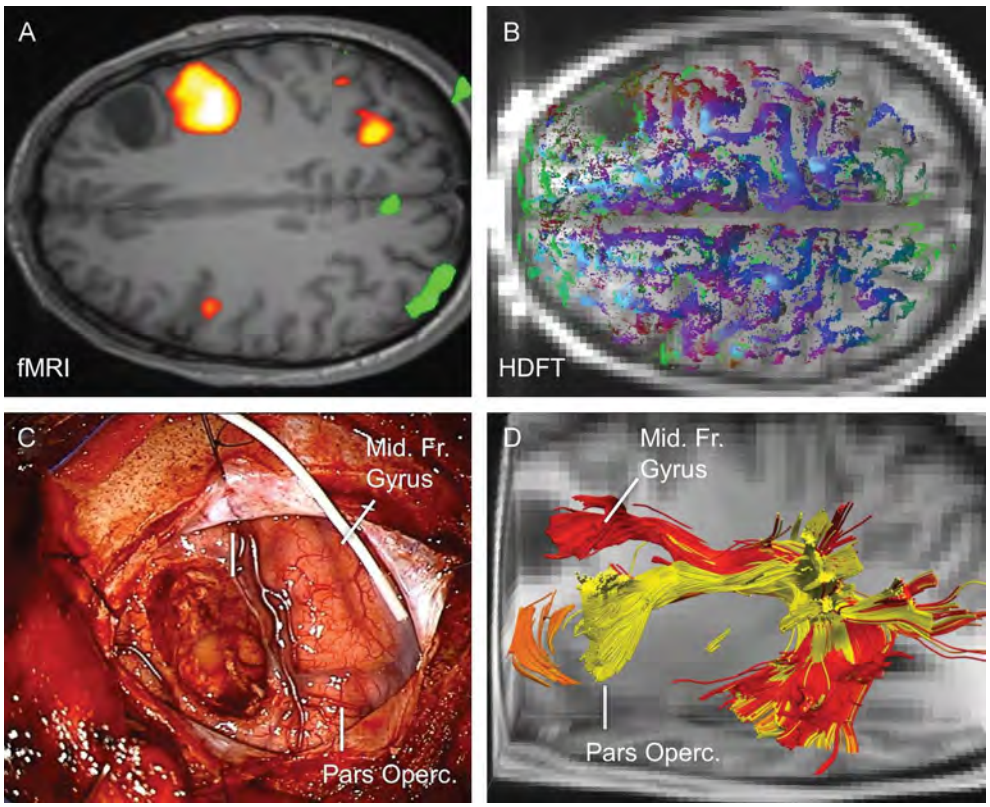

FIGURE 14. *Illustrative case 4. Left middle frontal (Mid. Fr.) gyrus low-grade glioma.* **A**, *functional magnetic resonance image (fMRI) showing activation just posterior to the tumor.* **B**, *high-definition fiber tractography (HDFT) of the end points of the whole brain fibers.* **C**, *intraoperative picture after resection of the tumor.* **D**, *HDFT of the cortical areas adjacent to the tumor. Operc., opercularis.*

series, HDFT has repeatedly shown the complete absence of fibers within the tumor substance. Interestingly, the fibers that would normally occupy the tumor space are displaced around in such a way that they form the macroscopic margins of the tumor. Anatomical location (for instance, precentral gyrus), functional imaging, and intraoperative cortical/subcortical stimulation provide functional assignment to the fiber tracts. Recent studies have provided evidence for the infiltration of the white matter in low-grade gliomas up to 2 cm beyond the fluid-attenuated inversion-recovery signal abnormality.[49] It is essential to note that microscopic infiltration of the fiber tracts cannot be evaluated with the HDFT technique presented here.

Our limited experience with diffuse low-grade gliomas suggests that, as with focal gliomas, there are no fibers within focal portions of the tumor (for instance, within a particular gyrus), but secondary to the diffuse expansion of the tumor, fiber tracts become trapped between focal portions of the tumor (for instance, in between adjacent gyri). These observations support the hypothesis that low-grade gliomas mostly grow in between the fibers tracts, following their same pathway, rather than within the fiber tracts.

CASE 3

A 50-year-old female patient presented to the hospital after a motor vehicle accident secondary to a focal motor seizure (right hemibody). On examination, a very mild right hemiparesis (4+/5) was identified, with more intense weakness on right foot dorsiflexion. Conventional MRI study showed a partially cystic intra-axial mass with mild focus of enhancement located in the left supplementary motor area (superior frontal gyrus) adjacent to the precentral gyrus. Presurgical HDFT was completed, showing a complete absence of fibers within the tumor. The fiber tracts were all displaced around the tumor to form the macroscopic margins of the lesion. The main stem of the cingulum was pushed downward, and the corticospinal tract was displaced posteriorly and laterally (Figure 13). As stated before, infiltration of these fiber tracts cannot be ascertained with current fiber tracking techniques. Subtotal surgical resection was undertaken using awake craniotomy with intraoperative cortical and subcortical stimulation that revealed positive motor responses at the posterior and posterior-inferior margins of the tumor as suggested by preoperative HDFT. Final diagnosis was gemistocytic astrocytoma World Health Organization

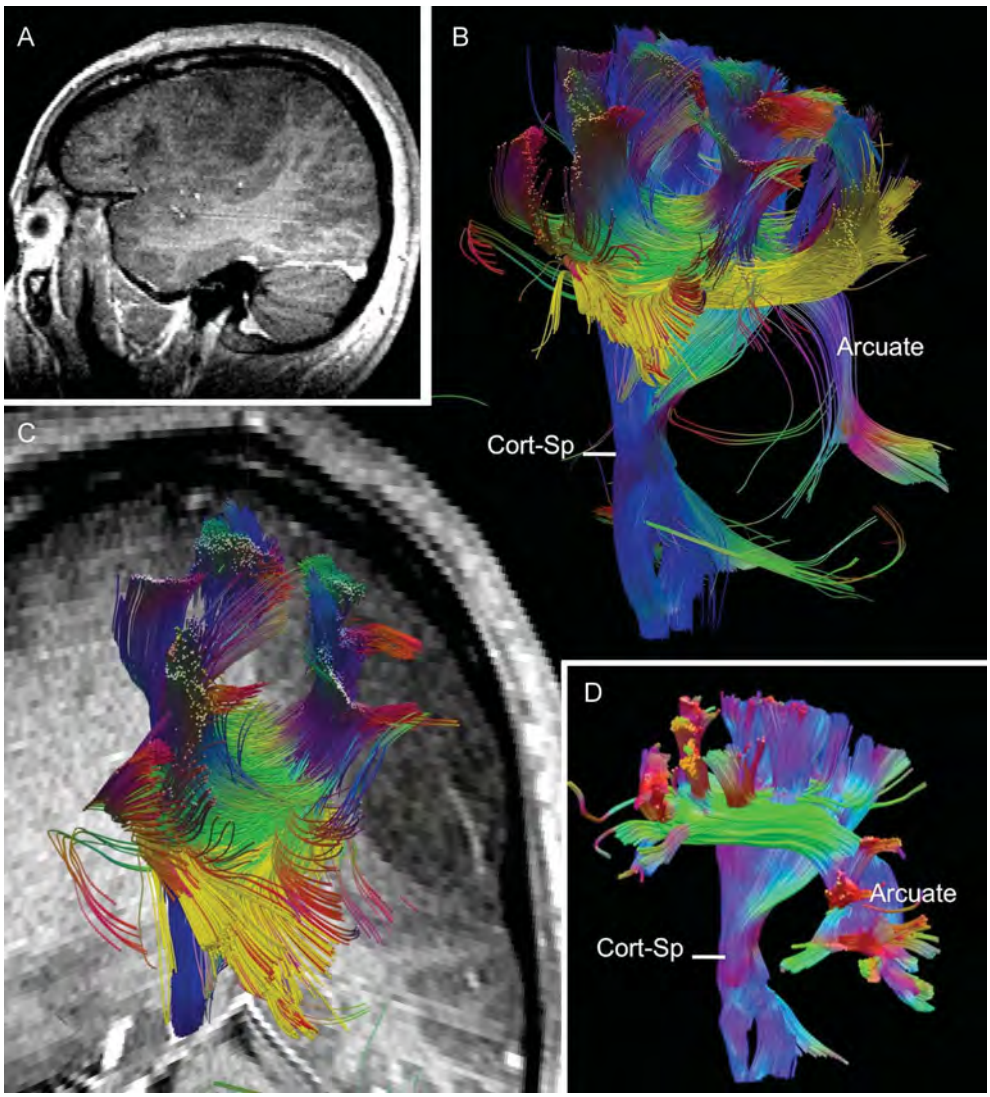

FIGURE 15. *Illustrative case 5. Diffuse left frontal low-grade glioma.* **A**, *structural magnetic resonance image, sagittal view.* **B**, *high-definition fiber tractography (HDFT) of the fibers within and around the tumor.* **C**, *close-up view showing the displacement of fibers caused by the tumor.* **D**, *HDFT of the arcuate and corticospinal (Cort-Sp) tracts to correlate with* **B** *and* **C**.

grade 2. The patient's motor examination remained at baseline. Conventional MRI at the 3-month follow-up showed evidence for residual tumor. Postoperative HDFT study showed resolution of the displacement of the corticospinal tract and cingulum fibers. Tumoral infiltration of these tracts, particularly the cingulum, cannot be ruled out.

Case 4

A 41-year-old right-handed male patient underwent an MR study after a seizure. A focal low-grade glioma was identified at the midportion of the left middle frontal gyrus (or dorsolateral prefrontal cortex). Functional MR revealed positive Blood Oxygen Level-Dependent signal for language task in the gyrus located immediately behind the tumor, an area that corresponds to the so-called ventral premotor cortex. The HDFT study confirmed the absence of fibers within the tumor and the displacement of fibers around the tumor with no fiber disruption. Because of the location of the tumor, we performed focused reconstruction of the arcuate tract. We identified 2 major groups of fibers that contributed to the formation of the arcuate tract, one arising from the ventral premotor cortex, just posterior to the tumor, and the second originating from pars opercularis, just inferior and posterior to the mass. During surgery, cortical stimulation of the ventral

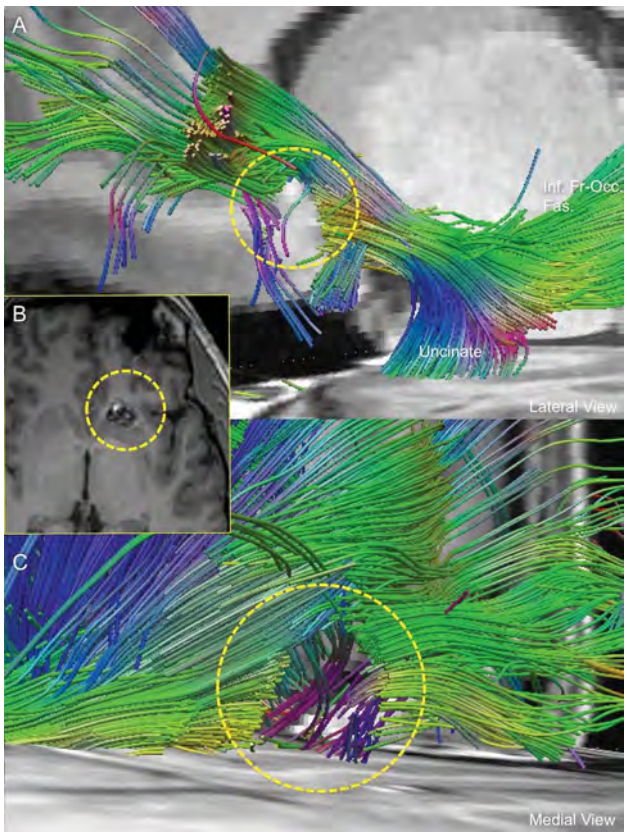

FIGURE 16. *Illustrative case 6. Uncinate fascicle cavernoma.* **A**, *high-definition fiber tractography (HDFT), lateral view.* **B**, *structural magnetic resonance image, axial cut.* **C**, *HDFT, medial view. Inf. Fr. Occ., inferior frontal occipital.*

premotor cortex elicited speech arrest (note that pars opercularis was not exposed and stimulated), confirming its role in the language system as part of the arcuate tract. Cortical stimulation of the dorsolateral prefrontal cortex (the tumor location) was negative (Figure 14).

Case 5

A 28-year-old male patient presented with an epileptic seizure but was otherwise asymptomatic. An MRI study showed a diffuse low-grade glioma infiltrating several gyri: inferior frontal gyrus (pars opercularis), posterior portion of the middle frontal gyrus, and most lateral portion of the precentral gyrus. The HDFT study showed displacement of the short intergyral fibers trapped within the tumor. The tumor appeared to follow the same pathway as the arcuate tract, but rather than disrupting this fiber tract, the tumor mass displaced down the main stem of the frontal portion of the arcuate tract and pushed away the branches of the arcuate tract that interconnect the inferior frontal gyrus (pars opercularis), posterior middle frontal gyrus, and lateral portion of the precentral gyrus. Complete resection of this tumor would entail resection of the trapped intergyral fibers and significant risk for arcuate tract damage. The pyramidal tract, however, appeared to be spared by the tumor. The patient underwent stereotactic frameless biopsy (Figure 15).

Cavernomas

Our HDFT studies on these vascular lesions have shown a complete absence of fibers within the cavernoma (as it is otherwise well known) and various degrees of fiber disruption and displacement. Remarkably, in hemorrhagic lesions, we have observed a predominance of fiber disruption over displacement, likely secondary to the acute bleeding event or events causing fiber breakage rather than the typical fiber deformation caused by subacute or chronic lesions such as the previously studied gliomas. When surgery for cavernoma removal is indicated, it becomes critical to discern the safest trajectory into the lesion. Consequently, accurate mapping of surrounding fiber tracts is of paramount importance to reduce surgical morbidity.

Case 6

A 53-year-old man presented with repeated seizures. The MRI study revealed a lesion compatible with a cavernoma located deep in the left orbitofrontal region, just in front of the caudate head and putamen and medial to the anterior insular sulcus. The patient had had 2 separate episodes of seizures and headaches, presumably related to cavernoma bleeding and expansion. Medical treatment had been effectively controlling seizures, but given the repeated hemorrhagic episodes, surgery was offered to the patient. Preoperative HDFT study showed clear disruption of the fibers coincidental with the location of the cavernoma; in fact, the fiber reconstruction helped to define better the anatomical location of the cavernoma: the proximal orbitofrontal segment of the uncinate fascicle. Detailed analysis revealed that the orbitofrontal fibers of the uncinate fascicle were disrupted. Several surgical routes were discussed, including the left transsylvian transinsular (through the anterior insular sulcus) approach, anterior interhemispheric fissure approach, anterior transfrontal approach, and anterior subfrontal approach. On the basis of the information provided by the HDFT study, the subfrontal route was selected to take advantage of the already established fiber damage and to avoid new fiber disruption with the surgical approach (Figure 16).

Case 7

A 23-year-old woman acutely presented with severe left hemiparesis, facial nerve palsy, and diplopia. An MRI showed an approximately 1-cm hematoma in the right pontomesencephalic region suggestive of an underlying brainstem cavernoma. Over the course of 2 weeks, she partially recovered from her neurological deficits, but a sudden neurological deterioration was associated with a new bleeding event. This time, the pontomesencephalic lesion measured $>$ 2 cm and occupied most of the right pontine region. The patient was transferred to our institution for surgical resection of the lesion. Presurgical HDFT was completed,

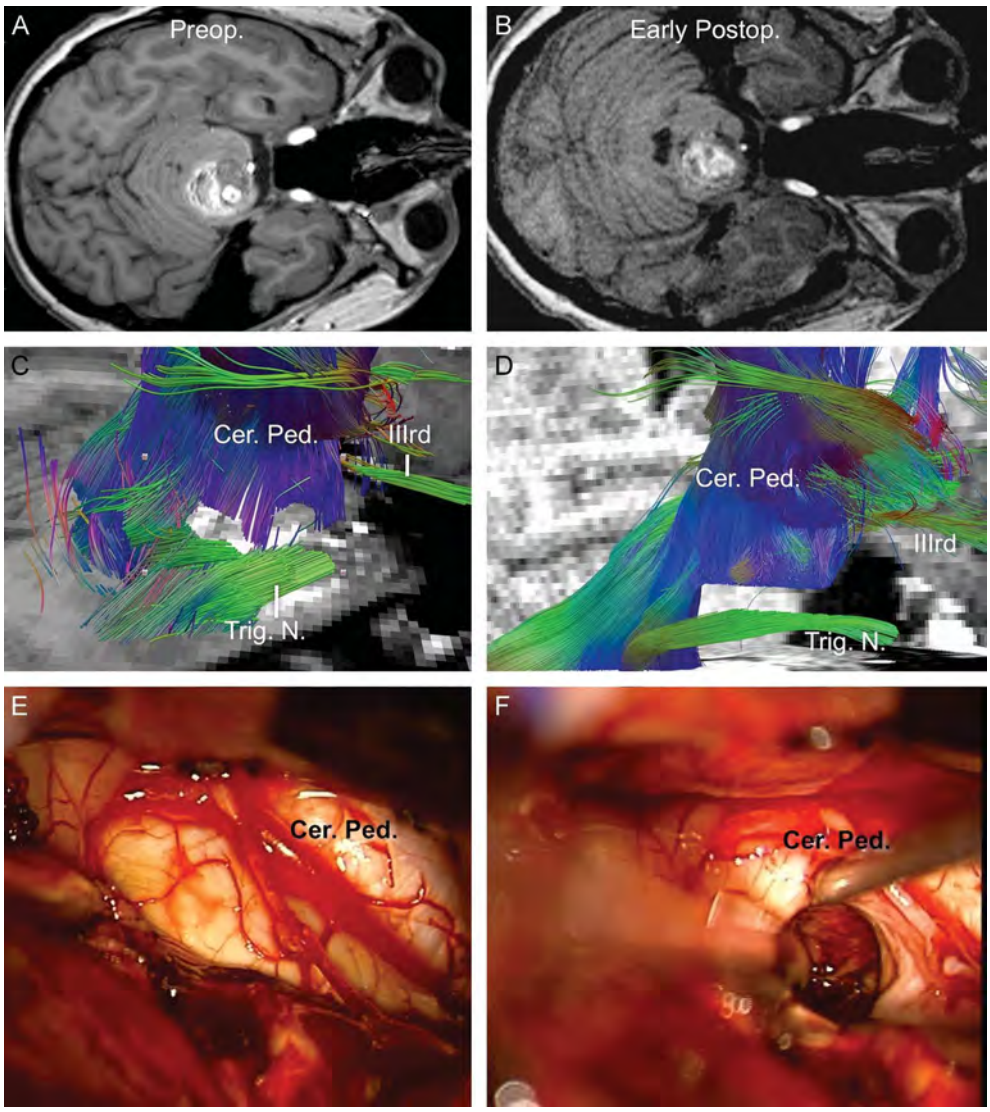

FIGURE 17. *Illustrative case 7. Pontomesencephalic cavernoma.* **A**, *preoperative structural magnetic resonance image (MRI), axial cut.* **B**, *early postoperative structural MRI, axial cut.* **C**, *preoperative high-definition fiber tractography (HDFT) showing the disruption of the cerebral peduncle (Cer. Ped.) caused by the cavernoma hemorrhage.* **D**, *early postoperative HDFT showing the clear disruption of the cerebral peduncle caused by the surgical entry. Note the straight cut on the cerebral peduncle fiber.* **E**, *intraoperative picture before the corticectomy; the lateral surface of the cerebral peduncle shows some hemosiderin coloration at the approximate location of the fiber disruption shown in C.* **F**, *intraoperative picture after the corticectomy to correlate with* **D**. *N. indicates nerve.*

evidencing severe disruption and displacement of the right corticospinal tract. Importantly, an area of disruption of the right corticospinal tract was identified at the lateral aspect of the cerebral peduncle, right above the trigeminal nerve and below the oculomotor nerve. This area of disruption was thought to be the ideal entry point into the brainstem through an anterior subtemporal transtentorial approach with anterior petrosectomy (Figures 17 and 18). It is critical to state that the preferred approach and surgical entry point for such a pontine cavernoma would have been the same regardless of the use of HDFT; the fiber tracking study did not change the approach but reinforced the planned strategy. When the brainstem was viewed from the front, the middle cerebellar peduncle appeared completely disrupted, the right corticospinal tract was severely displaced laterally with partial disruption, and the left corticospinal tract was mildly pushed laterally (Figures 17 and 19). We did not track

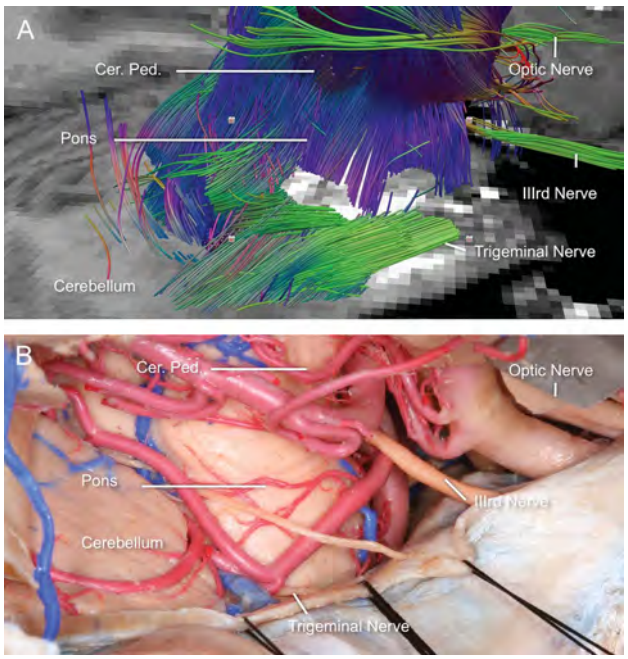

FIGURE 18. *Illustrative case 7 (continuation).* **A**, *close-up view of the preoperative high-definition fiber tractography study. Note the disruption of the cerebral peduncle (Cer. Ped.) and the accurate replication of the oculomotor and trigeminal cranial nerves.* **B**, *anatomical dissection in an injected specimen to correlate with* **A**.

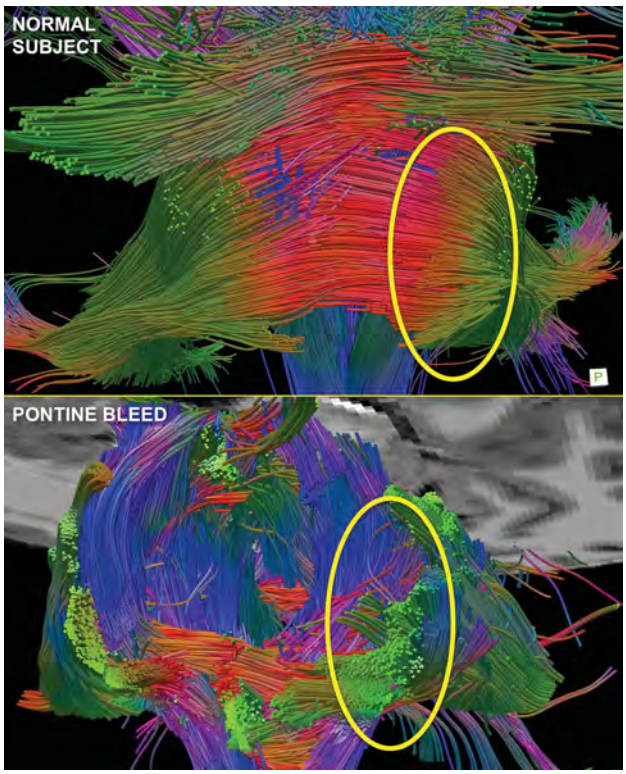

FIGURE 19. *Illustrative case 7 (continuation). High-definition fiber tractography of the pontine region in a normal subject (***top***) and the patient with the pontine cavernoma (***bottom***). The yellow oval highlights the disruption of the middle cerebellar peduncle.*

any fibers within the area of the hemorrhagic lesion. Interestingly, we performed HDFT studies in the early (3 weeks) and late (4 months) postoperative periods. The early study replicated with remarkable accuracy the brainstem corticectomy that gave access to the cavernoma and showed the relaxation on the corticospinal tracts. The late study served to evaluate the status of the corticospinal tracts, evidencing a 70% decrease in the density of the right corticospinal fibers (Figure 20). Despite this damage, the patient has made a remarkable recovery and is able to ambulate normally but with severe palsy in the left distal upper extremity.

DISCUSSION

We present our results applying HDFT to investigate the structure of the normal and pathological human brain. HDFT represents a significant improvement in MR-based fiber tracking techniques. The resolution of the crossing and termination problems is illustrated here with the accurate replication of known neuroanatomical features such as the gyral and sulcal folding pattern, the characteristic shape of the claustrum, the segmentation of the thalamic nuclei, the decussation of the superior cerebellar peduncle, the multiple fiber crossing at the centrum semiovale, the complex angulation of the optic radiations, the terminal arborization of the arcuate tract, and the cortical segmentation of the dorsal Broca area.

The impossibility of in vivo human neurohistological studies and the limited resolution of ex vivo studies for long axonal projections make animal studies with autoradiographic techniques the current gold standard for brain connectivity.[18,19] Mesulam stated: "There is currently no method that can come close to tracing connections in the human brain with the sort of precision described in this book. . .they [MR based tractography] have a long way to go before they can tell us the cells of origin, white matter trajectories, and termination fields of pathways emanating from cortical areas no larger than a few millimeters in size."[19] In this study, we show that HDFT is an effective deterministic method to study structural brain connectivity in the living human brain that allows us to follow fibers from their origin to their destination through complex crossings. Importantly, many regions of the human brain are significantly different from their monkey counterparts, so extrapolation of results from monkey studies could mislead the research in humans.[50] Therefore, we believe that HDFT will have a major role in building the structural network of the brain, the so-called human connectome.[51] The combination of HDFT and neuropsychological

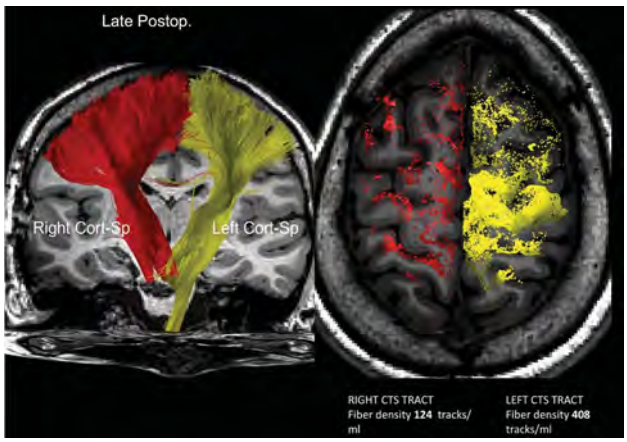

FIGURE 20. *Illustrative case 7 (continuation). Late postoperative high-definition fiber tractography study. Note the reduction of fiber end points at the right (red) motor trip compared with the left one (yellow). Cort-Sp, corticospinal.*

examinations, probabilistic tractography, and modalities of functional brain mapping such as electroencephalography, magnetoencephalography, direct stimulation (intraoperative or perioperative), and functional MRI could facilitate numerous structural/functional correlations of poorly understood fiber tracts.

The science of MR-based "connectomics" aims to understand the structural and functional details of brain networks.[52] Theoretically, once we develop the technology to map an individual connectome accurately and repeatedly, we will be able to investigate a broad spectrum of neurological, psychiatric, and even behavioral disorders. By referring to a database that contains information on multiple subjects, we will be able to describe the connectivity pattern of multiple neurological disorders such as autism and Alzheimer disease. We may even be able to account for personality variants and traits that differentiate one person from another.[53]

The dominance of cortical-based theories for explaining brain functioning has now shifted to a network-based or connectivity approach.[44,54] As we observe the cortical terminations of the fiber tracts, we realize that the afferent/efferent fibers may define a cortical area; therefore, the known variability of cortical regions may well be determined by the variability of their connection fibers. This inside-out approach (from the fiber tract to the cortical region) may explain, for instance, the variability and/or multiplicity on the location of the speech sensory center (Wernicke area). Correlating HDFT with intraoperative cortical mapping could test this hypothesis.

From a clinical perspective, we show here that accurate structural connectivity studies in patients facilitate white matter damage assessment, aid in understanding lesional patterns of white matter structural damage, and allow innovative neurosurgical applications. Regarding the assessment of fiber tract damage, we can clearly differentiate displacement from disruption of fibers. One common concern is whether the disruption of fibers is real. At this point, we have evidence (postoperative HDFT studies showing the expected surgical damage) that supports the accuracy of the technique to show real disruption; however, we do not know yet what the sensitivity of the technique is, in other words, what degree of fiber damage is enough to show up as fiber disruption and whether that damage is reversible. The question of reversibility is of major importance. The ability to accurately discern between reversible (presumably just displacement of fibers) and irreversible (disruption of fibers) damage would have strong prognostic implications and a significant impact on the decision-making process for surgical indication and rehabilitation therapy targeting. There is an urgent need to perform histological postmortem validation of HDFT fiber damage assessment in animal models.

From the results of our study, we may obtain a better understanding of the structural impact of gliomas. Logically, high-grade gliomas produce significant disruption of fibers, whereas low-grade gliomas cause fiber displacement. Remarkably, focal low-grade gliomas in our series did not show any coherent fibers within the tumor substance. But do diffuse low-grade gliomas grow within fiber tracts or rather in a parafascicular fashion? Our preliminary experience suggests that low-grade gliomas tend to grow following the parafascicular space displacing more than infiltrating the fiber tract. Further studies to validate the clinical findings are needed. In particular, correlation studies between preoperative HDFT, intraoperative cortical/subcortical stimulation, and postoperative HDFT are currently underway at our institution.

The use of HDFT for the presurgical analysis of structural damage provides more sophisticated information than current neuroimaging reports. A detailed qualitative and quantitative study of independent fiber tracts will complement and enrich the clinical and neuropsychological evaluation of patients with intracerebral lesions. Qualitative parameters such as tract thickness, branching pattern, and shape deformation and quantitative measurements such as number of streamlines, volume, and density of the fiber tract will become an integral part of the diagnostic evaluation of the patient. Furthermore, postoperative qualitative and quantitative evaluation of the fiber tracts will help us understand better the structural impact of surgery itself, disease progression, adjuvant therapies, and rehabilitation therapy.

MR-based fiber tracking techniques already have a well-established role in the presurgical planning process. However, limited resolution and multiple artifacts have reduced the applicability of the technique to a few easy-to-reconstruct fiber tracts such as the corticospinal tract.[55] In this report, we describe segmentation of multiple fiber tracts in the clinical setting, even in the presence of surrounding edema or large mass effect. From a practical point of view, we can now perform "computer-based dissection" (compared with anatomical fiber dissection) not only in normal subjects but also in patients with brain lesions; we can carefully investigate the complete network of fibers that surround an intracerebral lesion and simulate the fiber tracts that would be

crossed and severed using a particular surgical approach[56]; we can even take into account existing fiber damage to design the less invasive surgical approach (see illustrative cases 6 and 7).

Intraoperative neurophysiological techniques are currently considered the gold standard for cortical/subcortical mapping during tumor resection in eloquent areas.[44,46] However, these techniques have significant time constraints, have limited function examination (motor, language, vision), and are patient and operator dependant. We envision that matching HDFT with preoperative neurophysiological and/or functional neuroimaging techniques will allow accurate presurgical white matter mapping and, after its integration with reliable neuronavigation devices and intraoperative stimulation techniques, will become the gold standard for intracerebral tumor resection.

Limitations of the Technique

Despite the dramatic improvement in the fiber tracking technique presented here, the application of HDFT in the clinical setting should be performed with extreme caution and criticism. As mentioned before, validation of HDFT is needed both in animal models and in the clinical setting. Importantly, HDFT provides structural information based on the diffusion of axonal water, but it does not provide functional information per se. HDFT should not be used as the sole modality to make therapeutic decisions in any case and should always be considered a complement rather than an alternative to current imaging and surgical strategies. Similarly, the neuro-oncological principle of maximal and safe tumor resection should not be revised on the basis of HDFT results.

Several limitations prevent HDFT from becoming the gold standard in white matter anatomy studies. The false continuation problem is pending resolution. We are currently investigating the application of regional fiber tracking paradigms that adapt to the specific circumstances of certain anatomical regions to reduce artifacts and pseudotracts. The false continuation problem is directly related to the current spatial resolution of MR voxel sixe (1-2 mm^3). This will improve with implemented magnets. The head movement problem has been partially solved with the introduction of a novel prosthesis that fixates the head in neutral position. Collaboration of the patient is critical and, unfortunately, impossible in some patients with behavioral issues. We have seen a strong influence of head movement in the final quality of the fiber tracking data, so the importance of avoiding any movement during the scanning process cannot be underestimated. Along the same lines, reducing the scanning time, currently around 45 minutes, requires further research efforts to facilitate clinical application. Finally, it is well known that changing the fiber tracking parameters such as fractional anisotropy value influences the end product of the fiber reconstruction. Our criteria will always follow strict neuroanatomy judgment: The right fiber tracking parameters are those that will replicate known neuroanatomical features as presented here. It is critical to stress the importance of the neuroanatomy quality test for fiber tracking techniques, and we are convinced that the selected features presented here are necessary but not sufficient to achieve the ultimate goal of fiber tracking techniques: clinically efficient in vivo quasihistological precision.

Disclosures

This work was supported by The Copeland Fund of the Pittsburgh Foundation (2009-2010 and 2010-2011). The authors have no personal financial or institutional interest in any of the drugs, materials, or devices described in this article.

REFERENCES

1. Crick F, Jones E. Backwardness of human neuroanatomy. *Nature*. 1993;361(6408):109-110.
2. Basser PJ, Pajevic S, Pierpaoli C, Duda J, Aldroubi A. In vivo fiber tractography using DT-MRI data. *Magn Reson Med*. 2000;44(4):625-632.
3. Mori S. Two and three-dimensional analyses of brain white matter architecture using diffusion imaging. *CNS Spectr*. 2002;7(7):529-534.
4. US Department of Health and Human Services. NIH news. Available at: http://www.nih.gov/news/health/jul2009/ninds-15.htm. Accessed August 6, 2009.
5. Catani M, Howard RJ, Pajevic S, Jones DK. Virtual in vivo interactive dissection of white matter fasciculi in the human brain. *Neuroimage*. 2002;17(1):77-94.
6. Fernandez-Miranda JC, Rhoton AL Jr, Alvarez-Linera J, Kakizawa Y, Choi C, de Oliveira E. Three-dimensional microsurgical and tractographic anatomy of the white matter of the human brain. *Neurosurgery*. 2008;62(6 suppl 3):989-1028.
7. Nimsky C, Ganslandt O, Merhof D, Sorensen AG, Fahlbusch R. Intraoperative visualization of the pyramidal tract by diffusion-tensor-imaging-based fiber tracking. *Neuroimage*. 2006;30(4):1219-1229.
8. Nimsky C, Ganslandt O, Fahlbusch R. Implementation of fiber tract navigation. *Neurosurgery*. 2006;58(4 suppl 2):ONS292-ONS304.
9. Nimsky C, Ganslandt O, Hastreiter P, Wang R, Benner T, Sorensen AG, Fahlbusch R. Preoperative and intraoperative diffusion tensor imaging-based fiber tracking in glioma surgery. *Neurosurgery*. 2005;56(1):130-138.
10. Berman JI, Berger MS, Mukherjee P, Henry RG. Diffusion-tensor imaging-guided tracking of fibers of the pyramidal tract combined with intraoperative cortical stimulation mapping in patients with gliomas. *J Neurosurg*. 2004;101(1):66-72.
11. Kamada K, Todo T, Masutani Y, et al. Combined use of tractography-integrated functional neuronavigation and direct fiber stimulation. *J Neurosurg*. 2005;102(4):664-672.
12. Kamada K, Sawamura Y, Takeuchi F, et al. Functional identification of the primary motor area by corticospinal tractography. *Neurosurgery*. 2005;56(1 suppl):98-109.
13. Kamada K, Todo T, Morita A, et al. Functional monitoring for visual pathway using real-time visual evoked potentials and optic-radiation tractography. *Neurosurgery*. 2005;57(1 suppl):121-127.
14. Kamada K, Todo T, Masutani Y, et al. Visualization of the frontotemporal language fibers by tractography combined with functional magnetic resonance imaging and magnetoencephalography. *J Neurosurg*. 2007;106(1):90-98.
15. Henry RG, Berman JI, Nagarajan SS, Mukherjee P, Berger MS. Subcortical pathways serving cortical language sites: initial experience with diffusion tensor imaging fiber tracking combined with intraoperative language mapping. *Neuroimage*. 2004;21(2):616-622.
16. Alexander DC, Barker GJ. Optimal imaging parameters for fiber-orientation estimation in diffusion MRI. *Neuroimage*. 2005;27(2):357-367.
17. Le Bihan D, Poupon C, Amadon A, Lethimonnier F. Artifacts and pitfalls in diffusion MRI. *J Magn Reson Imaging*. 2006;24(3):478-488.
18. Johansen-Berg H, Rushworth MF. Using diffusion imaging to study human connectional anatomy. *Annu Rev Neurosci*. 2009;32(3):75-94.
19. Schmahmann JD, Pandya DN. *Fiber Pathways of the Brain*. New York, NY: Oxford University Press; 2006.
20. Provenzale JM, McGraw P, Mhatre P, Guo AC, Delong D. Peritumoral brain regions in gliomas and meningiomas: investigation with isotropic diffusion-weighted MR imaging and diffusion-tensor MR imaging. *Radiology*. 2004;232(2):451-460.
21. Jansons KM, Alexander DC. Persistent angular structure: new insights from diffusion magnetic resonance imaging data. *Inf Process Med Imaging*. 2003;18:672-683.

22. Wedeen VJ, Hagmann P, Tseng WY, Reese TG, Weisskoff RM. Mapping complex tissue architecture with diffusion spectrum magnetic resonance imaging. *Magn Reson Med*. 2005;54(6):1377-1386.
23. Schmahmann JD, Pandya DN, Wang R, et al. Association fibre pathways of the brain: parallel observations from diffusion spectrum imaging and autoradiography. *Brain*. 2007;130(pt 3):630-653.
24. Walt Schneider Research Lab. Pittsburgh Brain Competition 2009. Available at: http://pbc.lrdc.pitt.edu. Accessed August 15, 2009.
25. Yeh FC, Wedeen VJ, Tseng WY. Generalized q-sampling imaging. *IEEE Trans Med Imaging*. 2010;29(9):1626-1635.
26. DSI studio. Available at: http://dsi-studio.labsolver.org. Accessed June 7, 2010.
27. Yeh FC, Wedeen VJ, Tseng WY. Estimation of fiber orientation and spin density distribution by diffusion deconvolution. *Neuroimage*. 2011;55(3):1054-1062.
28. Verstynen T, Jarbo K, Pathak S, Schneider W. In vivo mapping of microstructural somatotopies in the human corticospinal pathways. *J Neurophysiol*. 2011;105(1):336-346.
29. Shin SS, Verstynen T, Pathak S, et al. High-definition fiber tracking for assessment of neurological deficit in a case of traumatic brain injury: finding, visualizing, and interpreting small sites of damage. *J Neurosurg*. 2012;116(5):1062-1069.
30. Jarbo K, Verstynen T, Schneider W. In vivo quantification of global connectivity in the human corpus callosum. *Neuroimage*. 2012;59(3):1988-1996.
31. Pathak S, Fissell C, Jung KJ, Schneider W. Diffusion weighted MRI, comparison study of reconstruction and fiber tracking algorithms, and related tools. Presented at: Organization of Human Brain Mapping; June 10-14, 2007; Chicago, IL.
32. Lazar M, Weinstein DM, Tsuruda JS, et al. White matter tractography using diffusion tensor deflection. *Hum Brain Mapp*. 2003;18(4):306-321.
33. *TrackVis*. Available at: http://trackvis.org. Accessed January 27, 2009.
34. Ludwig E, Klingler J. *Atlas Cerebri Humani: The Inner Structure of the Brain Demonstrated on the Basis of Macroscopical Preparations*. Boston, MA: Little Brown and Co; 1956.
35. Crick FC, Koch C. What is the function of the claustrum? *Philos Trans R Soc Lond B Biol Sci*. 2005;360(1458):1271-1279.
36. Fernandez-Miranda JC, Rhoton AL Jr, Kakizawa Y, Choi C, Alvarez-Linera J. The claustrum and its projection system in the human brain: a microsurgical and tractographic anatomic study. *J Neurosurg*. 2008;108(4):764-774.
37. Nieuwenhuis R, Voogd J, van Huizen C. *The Human Central Nervous System*. 4th ed. Berlin, Germany: Springer-Verlag; 2008.
38. Behrens TE, Johansen-Berg H, Woolrich MW, et al. Non-invasive mapping of connections between human thalamus and cortex using diffusion imaging. *Nat Neurosci*. 2003;6(7):750-757.
39. Choi C, Rubino PA, Fernandez-Miranda JC, Abe H, Rhoton AL Jr. Meyer's loop and the optic radiations in the transsylvian approach to the mediobasal temporal lobe. *Neurosurgery*. 2006;59(4 suppl 2):ONS228-ONS235.
40. Catani M, Mesulam M. The arcuate fasciculus and the disconnection theme in language and aphasia: history and current state. *Cortex*. 2008;44(8):953-961.
41. Glasser MF, Rilling JK. DTI tractography of the human brain's language pathways. *Cereb Cortex*. 2008;18(11):2471-2482.
42. Makris N, Kennedy DN, McInerney S, et al. Segmentation of subcomponents within the superior longitudinal fascicle in humans: a quantitative, in vivo, DT-MRI study. *Cereb Cortex*. 2005;15(6):854-869.
43. Fernandez-Miranda JC, Pathak S, Schneider W. High-definition fiber tractography and language. *J Neurosurg*. 2010;113(1):156-157.
44. Duffau H. New concepts in surgery of WHO grade II gliomas: functional brain mapping, connectionism and plasticity: a review. *J Neurooncol*. 2006;79(1):77-115.
45. Schiffbauer H, Ferrari P, Rowley HA, Berger MS, Roberts TP. Functional activity within brain tumors: a magnetic source imaging study. *Neurosurgery*. 2001;49(6):1313-1320.
46. Sanai N, Berger MS. Intraoperative stimulation techniques for functional pathway preservation and glioma resection. *Neurosurg Focus*. 2010;28(2):E1.
47. Chang EF, Clark A, Smith JS, et al. Functional mapping-guided resection of low-grade gliomas in eloquent areas of the brain: improvement of long-term survival: clinical article. *J Neurosurg*. 2011;114(3):566-573.
48. Mandonnet E, Capelle L, Duffau H. Extension of paralimbic low grade gliomas: toward an anatomical classification based on white matter invasion patterns. *J Neurooncol*. 2006;78(2):179-185.
49. Pallud J, Varlet P, Devaux B, et al. Diffuse low-grade oligodendrogliomas extend beyond MRI-defined abnormalities. *Neurology*. 2010;74(21):1724-1731.
50. Rilling JK, Glasser MF, Preuss TM, et al. The evolution of the arcuate fasciculus revealed with comparative DTI. *Nat Neurosci*. 2008;11(4):426-428.
51. Hagmann P, Cammoun L, Gigandet X, et al. Mapping the structural core of human cerebral cortex. *PLoS Biol*. 2008;6(7):e159.
52. Hagmann P, Cammoun L, Gigandet X, et al. MR connectomics: principles and challenges. *J Neurosci Methods*. 2010;194(1):34-45.
53. Sporns O. The human connectome: a complex network. *Ann N Y Acad Sci*. 2011;1224(4):109-125.
54. Mesulam MM. Large-scale neurocognitive networks and distributed processing for attention, language, and memory. *Ann Neurol*. 1990;28(5):597-613.
55. Golby AJ, Kindlmann G, Norton I, Yarmarkovich A, Pieper S, Kikinis R. Interactive diffusion tensor tractography visualization for neurosurgical planning. *Neurosurgery*. 2011;68(2):496-505.
56. Fernandez-Miranda JC, Engh JA, Pathak SK, et al. High-definition fiber tracking guidance for intraparenchymal endoscopic port surgery. *J Neurosurg*. 2010;113(5):990-999.

Acknowledgments

The authors would like to thank Denise Davis for her invaluable job coordinating the MRI studies and Wendy Fellows for her help in the Surgical Neuroanatomy Laboratory. Dr Fernandez-Miranda deeply appreciates the continuous support provided by Maria Bolado, Blanca, and Martin to complete this project.